

**ATOLL RESEARCH BULLETIN
NO. 366**

**CHAPTER 2
CHARACTERISTICS OF OCEANOGRAPHIC PROCESSES ON REEFS
OF THE SEYCHELLES ISLANDS**

BY

**A. V. NOVOZHILOV, Y. N. CHERNOVA, I. A. TSUKUROV,
V. A. DENISOV AND L. N. PROPP**

**ISSUED BY
NATIONAL MUSEUM OF NATURAL HISTORY
SMITHSONIAN INSTITUTION
WASHINGTON, D.C., U.S.A.
June 1992**

CHAPTER 2
CHARACTERISTICS OF OCEANOGRAPHIC PROCESSES ON REEFS
OF THE SEYCHELLES ISLANDS

BY

A. V. Novozhilov*, Y. N. Chernova, I. A. Tsukurov***, V. A. Denisov*, L.N. Propp***

INTRODUCTION

Tropical reef ecosystems are formed under conditions of complex variability of physical-chemical environmental factors. The shape of coral reefs depends to a great extent on the pattern of surface currents (Brown and Dunne 1980). Underwater geomorphological features of reef slopes and plateaus (buttress and reef-flat systems) abounding in spurs, coral columns, hollows, channels and tunnels are primarily the result of abrasive wave forces (Munk and Sargent 1954, Storr 1964, Mergner and Schuhmacher 1974). *In situ* measurements and aerial photography have revealed the existence of areas of vortex formation near islands with fringing reefs as well as zones with strong currents that affect the accumulation of sediments and development of benthic communities (Murray and Roberts 1977, Hamner and Hauri 1981, Roberts et al. 1981). Investigations of the complex reefs of Nicaragua and Barbados Island, conducted by Roberts and co-workers, (Roberts et al. 1975, 1977, Roberts and Suhayda 1977, Suhayda and Roberts 1977) determined the spatial zonation of hydrodynamic processes on a reef slope, the power contribution of different currents and sea states and the degree of dissipation of water motion on different reef sites. Other researchers (Von Arx 1948, Frith 1981, Wolanski 1981) showed the effects of wind drift, roughness, long gravity waves, upwelling and coastal sewage on the structure of currents and thermohaline conditions inside reef lagoons. Some authors (Storr 1964, Mergner and Schuhmacher 1974) stress that wave and current action are the main factors causing biotic zonation of patterns on coral reefs.

Water exchange processes provide reef areas with seawater circulation, thermal exchange and salt transport. The period during which the seawater in atoll lagoons is completely changed may range from several months to several years depending on the lagoon size and circulation speed (Gallagher et al. 1971, Stroup and Mayers 1974, Magnier and Wanthly 1976.) The degree of openness of lagoons produces important hydrological consequences that affect primary productivity. Considerable openness of a lagoon, for example, reduces the range of salinity variations, promotes development of greater biomasses and diversity of phytoplankton which leads to a high concentration of dissolved oxygen (Kwei 1977).

The distribution of major nutrients, such as phosphorus, nitrogen and silicon, are among the factors limiting the primary production of reef systems. For coral islands, the degree of enrichment of waters with nutrients depends on hydrodynamic factors such as: tidal and drift currents, internal inner waves and upwelling (Konnov and Scherbinin 1975, Gusev et al. 1980, Wolanski and Pickard

* Institute of Marine Biology, Far East Branch, USSR Academy of Sciences, Vladivostok, 690032, USSR

** Institute of Geography, Far East Branch, USSR Academy of Sciences, Vladivostok, 690032, USSR

*** All-Union Institute of Fishery and Oceanography, Moscow, USSR

1983). Biological nitrogen fixation (Hatcher and Hatcher 1981, Smith 1983), inclusion of organic nitrogen fixation and phosphorus into the production cycle through bacterioplankton, periphyton and filter-feeding animals (Sorokin 1977, 1986, Atkinson 1981) are intrinsic sources of nutrients. Partially closed cycles of nutrients within symbiotic animals such as molluscs and corals (Sorokin 1986) that dominate benthic production, result in nutrient ratios that differ from Redfield's ratio of C:N:P = 550:30:1. This enables the fixation of more organic carbon per unit of biomass than in planktonic systems (Smith 1983), even in waters depauperate in nitrogen and phosphorus.

STUDY AREA

During the northeastern monsoon conditions (November-March), the Seychelles Plateau is under the influence of the inter-tradewind equatorial counter-current which runs eastward. According to the data of different authors, the south boundary of this current in December-January is variable and ranges between about 8-10°S (Burkov 1982, Marsac et al. 1983, Potier and Marsac 1984). To the south, there is a south trade-wind current which crosses the Indian Ocean in a westerly direction. During winter, the axis of this current, where speeds are highest, lies at approximately 10°S (Burkov and Neyman 1977). A tropical front is situated between these opposing currents (7-12°S). This zone separates surface waters of low salinity, but high oxygen levels, of the northern Indian Ocean (Burkov 1982). The frontal boundary changes its position depending on climatic conditions during different years. The result is an increase in complexity of interannual and intraannual current patterns and areas of divergence and convergence that result in the upwelling of deep waters and the thickening of surface water layers, respectively, near the Seychelles Islands.

Vertical temperature structure of waters over shallow bottom sites consists of two layers. The surface layer is homogeneously warmed up to 27-30°C and its thickness is usually 30-40 m but may be as shallow as 20 m (Marsac and Hallier 1985). Deeper subsurface south subtropical intermediate water has a temperature of 12-14°C and a temperature gradient of 2.2 to 2.4°C per 10 m (Marsac and Hallier 1985). The investigations carried out in January near the equator revealed the existence of temperature fluctuations with a 2 h period and vertical amplitude of oscillation up to 40 m which become greater in the regions of intensive currents and at the upper boundaries of seasonal thermoclines (depth 105-115 m). Short-term fluctuations of temperature with a wave-like nature (amplitude of up to 7 m, Morozov et al. 1977) also were found.

Under southeastern monsoon conditions, equatorial counter-current waters have high salinities, while the south tradewind current shows lower salinities (Burkov and Neyman 1977). Subsurface south subtropical intermediate waters have high salinities since they are formed in a subtropical zone where evaporation exceeds precipitation. Additionally, transformed high salinity water of the subsurface Arabian intermediate water mass (more than 36.5 ppt.), is found (Burkov 1982) near 10°S latitude and running along the equator from the west. During the expedition, three morphological types of island system were investigated: (a) granitic islands with fringing reefs (Mahé, Praslin, La Digue); (b) sandy islands with platform reefs (Providence, African Banks, Desroches, Cœtivy) and (c) atolls (Farquhar, St. Joseph, Aldabra, Astove, Cosmoledo).

METHODS AND MATERIALS

Currents

Currents were recorded by recording current meters, both in the water column and in the bottom layer 0.5 m above the bottom. The interval of measurements was 15 min, and the duration of a recording ranged from 17 h to 8.5 days. Table 1 summarizes the descriptive characteristics of the sta-

tions. In addition to the hydrological investigations, hourly observations of wave and wind conditions were recorded for 24 h periods.

To estimate the structure, direction and speed of currents, a distribution density of direction probability function ($P=y$) and of modulus of current speed ($P=v$) (Bishev et al. 1977) were used. Turbulent features of water currents were estimated using a number of indices calculated for meridional (u) and zonal (v) components of a current velocity vector, including turbulence intensity, coefficients of horizontal turbulent exchange and coefficients of horizontal turbulent exchanges per hour. Intensity of turbulence ($J_{u,v}$) is a ratio of the quadratic mean deviations of rate pulsations to the average current rate. According to the tensor theory of turbulence, coefficients of horizontal turbulent exchange calculated by the method of Ertel-Shtokman (Ertel 1932, Shtokman 1940) represent the process of exchange of motion quality as an ellipse. The major axis corresponds to A_{\min} , the minor axis to A_{\max} . The ratio A_{\max}/A_{\min} determines the degree of anisotropy of horizontal turbulent exchange (ϵ).

To reveal the effect of different scale vortices on the processes of horizontal turbulent exchange, the series of rate components were averaged before treatment using a cosine filter periods of averaging (T_o) of 2, 6, 12, 24, 48 and 96 h (Ozmidov 1968). The structure of water flow and contribution of different scale vortices to turbulent energy were estimated using calculations (S_w). Reliability of the function maxima was determined at the 95% confidence interval.

Thermohaline structure, salinity and hydrochemical characteristics

Temperature, salinity and hydrochemical characteristics of waters were recorded at 24 coastal hydrological stations and on transects across major geomorphological zones of reef shallows. Separate hydrological sampling was conducted down to 200 m beyond the intertidal zone to record temperature, salinity, pH and dissolved oxygen. A water quality monitor and bathythermographs Tsurumi Seki, (model 2) were used in addition to a portable TS-probe and portable thermo-oxygenometer Watanabe Keiki Mgf.

Water samples for determinations of nutrient concentration were collected using bathometers, a submersible pump and SCUBA divers. Concentrations of phosphorus (general, inorganic and organic), nitrogen (ammonium, nitrite, nitrate and organic) and dissolved silicon were analyzed. The interval between sampling was 3 h, and samples for nutrient determination were taken every 6 h according to the phases of a given tidal cycle.

Samples were analyzed using the modifications of methods adopted in Strickland and Parsons (1972). Ammonium, phosphorus and nitrites were determined spectrophotometrically, nitrates were reduced to nitrites in a capillary column containing copper wire covered with cadmium layer (Anon. 1979). Silicon was determined by the improved method using ascorbic acid as a reducer, whereas organic nitrogen and phosphorus were analyzed according to the methods of Walderrama (1981).

A photometer with a silicon photodiode was used to estimate the vertical distribution of light in the water column. Spectral characteristics of sensitivity were determined by a filter having maximum penetration in the range of 550 nm. Measuring illumination in water, we at the same time controlled outward illumination. Obtained data were used to calculate light indices (K) according to Jerlov (1980).

RESULTS AND DISCUSSION

Fringing reefs of granitic islands (Mahé, Praslin and La Digue Islands).

Coastal reefs redistribute wave energy and redirect currents from the open sea into shallow waters. Water exchange is most intensive at the outer edge of a reef crest in the area of strong wave and current influence.

Station 10, near the south coast of Praslin Island, is subjected to the effects of a strong southeasterly current with periodic tidal reversals (Table 2) Mean current speeds are 17-21 $\text{cm}\cdot\text{sec}^{-1}$, maximal speeds reach 28-32 $\text{cm}\cdot\text{sec}^{-1}$. This current shows a high degree of stability ($J_{v,u} = 0.36-0.50$) under horizontal turbulent exchange ($A_{\text{max}} = 10^4-10^6 \text{cm}^2\cdot\text{sec}^{-1}$).

At sites protected from wave action, movement of water near the bottom becomes progressively weaker. At the western point of St. Anse Bay, *Sargassum* communities were exposed to weak unstable flows ($J_{v,u} = 8.5-9.4$) and typical current speeds over the bottom did not exceed 2-4 $\text{cm}\cdot\text{sec}^{-1}$. Horizontal turbulence also was weak at this site, on the average about 42 times weaker than in the open subtidal zone (Table 2).

Stronger coastal currents are typical of shallow bottom sites between islands. For example, the northeasterly flow between Cerf and St. Anne Islands ranged between 15 and 22 $\text{cm}\cdot\text{sec}^{-1}$. (Fig. 1, Table 2). On the average, turbulent flow during the northwesterly flow was higher ($A_{\text{max}} = 2\cdot 10^5 \text{cm}^2\cdot\text{sec}^{-1}$; $J_{v,u} = 1.13-1.35$) than that of the northeasterly one ($A_{\text{max}} = 1.6\cdot 10^5 \text{cm}^2\cdot\text{sec}^{-1}$; $J_{v,u} = 0.42-0.50$).

Turbulent processes over fringing reef platforms depend on energy mainly from tidal, drift and wave currents (Fig. 2). At most of the open sites (e.g., Praslin Island, St. 10) some influx of turbulent energy was documented even over averaging periods of more than 12 h, probably dependent on the effects of large scale oceanic circulation. The structure of pulsations in current speeds depends on tidal processes with typical periods of 12 and 6 h, wind drift effects with a period of about 24 h and other weather-related variations with 40-45 h periods (Fig. 3). High-frequency current fluctuations are probably due to orographical vortex formation and wave currents with 1-3 h periods.

Horizontal turbulent exchange in the areas studied is anisotropic due to its intensity (Table 2). The direction of maximal exchange approaches that of a dominating flow. For the same reason, the vortex structure of water motion near Mahé and Praslin is most clearly displayed as a spectrum of zonal components of current speeds, thermohalinic conditions, hydrochemical features and optical characteristics.

Thermohaline conditions, hydrochemical and optical characteristics.

The surface equatorial waters near the south coast of Praslin Island showed daily temperatures ranging from 28.3 to 29.7°C and daily salinities from 35.05 to 35.17 ppt. During the absence of intensive wind mixing, temperature and salinity characteristics depend on insolation. The maximum temperature (29.7°C) in the surface layers was observed at 1700 hrs local time, the minimum (28.6°C) occurred at 1500-1800 hrs. During the daytime, intensive evaporation from the surface caused formation of a more saline layer (up to 35.2-ppt) which sank to lower levels and became cooler at night. Tidal mixing equalized thermohaline parameters throughout the water column.

Values of pH ranged between 8.3 and 8.4. Dissolved oxygen concentrations varied from 101 to 108% of saturation (Fig. 4C). The maximum near the bottom (107%) was observed in the afternoon

and the minimum (101%) occurred during night and early morning hours, consistent with daily fluctuations of photosynthetic activity. Oxygen concentrations in the surface waters ranged from 104 to 108% during 24 h, with maxima at 400 hrs and minima at 1000 hrs.

Near La Digue Island, the salinity was somewhat higher (35.23 - 35.31 ppt) and off the south coast temperatures of the surface waters and near the bottom did not vary greatly between 1400-1600 hrs local zone time (28.1°C at 15-30 m to 28.4°C at the surface). The dissolved oxygen concentration was similar in absolute values (4.52-5.06 mg·l⁻¹) to that observed near Praslin Island (102.2-112.2% of saturation), whereas pH values ranged between 8.32 and 8.38.

A change in the optical type of the waters near Praslin Island occurred at 3 m in depth, with the surface layers corresponding to the type III coastal waters (K=0.200). Water layers deeper than 3 m corresponded to the type II oceanic waters (K=0.094).

Nutrient concentrations near Mahé, Praslin and La Digue Islands ranged within the following limits: phosphates in the surface waters ranged from 0.07 to 0.35 $\mu\text{g atom}\cdot\text{l}^{-1}$; organic phosphorus - 0.04 to 0.22; silicon 1.6 - 3.0; nitrites 0 - 2.0; nitrates 0 - 0.55; ammonia 0 - 3.0; and organic nitrogen 5.4 - 23.0. Near Praslin Island, under conditions of good water exchange, concentrations of phosphorus and silicon were constant throughout the water column down to 23-25 m. Waters near Victoria Harbor (Mahé Island) were the richest in nutrients and contained the highest phosphate and silicon concentrations (Table 3). Lower phosphate and nitrogen concentrations were recorded in the waters of Praslin and La Digue Island. Nitrites were not found near these islands, and nitrates and ammonia were observed only in the surface waters or at intertidal sites where seagrasses and algae grew. At low tide, regenerative capacity in the bottom sediments was indicated by considerable amounts of ammonia (up to 3 $\mu\text{g atom}\cdot\text{l}^{-1}$ - in bottom Cœtivy layers) where the concentration of organic nitrogen dropped from 15 to 8 $\mu\text{g atom}\cdot\text{l}^{-1}$. An increase in concentration of all nitrogen forms was observed southwards from Victoria Harbor (Mahé Island): nitrites from 0.10 to 0.13 $\mu\text{g atom}\cdot\text{l}^{-1}$; nitrates 0.36 - 0.55; and organic nitrogen 14.4 - 23.0. On the whole, the richest nutrient waters were observed in the most developed portions of the eastern and southeastern coasts of Mahé subjected to the effects of coastal sewage. The least nutrient concentrations were found in the waters of La Digue Island which is situated at the edge of a granitic fragment where there is a good exchange with oligotrophic oceanic waters.

Reefs of sandy islands (Cœtivy, African Banks, Providence, Desroches)

Cœtivy, Providence and African Banks have similar bottom topographies. They arise as wave swept sandy bedforms on shallow platforms of coral origin which form on top of underwater mountain ranges. Their coasts are fringed with coral-dominated reefs in different developmental stages and their platforms are covered with patches of coral communities and macrophytes. The nearshore circulation surrounding these islands have high hydrodynamic activity. During the present study, the east coast of Cœtivy Island was subjected to a strong northeastern current (Fig. 5, St. 2). Mean flow speeds in the upper 10 m layer of water were 34-42 cm·sec⁻¹ and deeper (30 m) they reached 44-63 cm·sec⁻¹ with maximal pulses 1 m·sec⁻¹ or more. Southeast of the South Island of African Banks at the seaward edge of a vast underwater terrace (St. 14) a strong eastward current with a mean speed of about 30 cm·sec⁻¹ was recorded. High current energy at the edges of island platforms results in the development of considerable turbulence. Thus, the coefficients of horizontal turbulent exchange near Cœtivy Island and African Banks ranged from 10⁴ to 10⁶ cm²·sec⁻¹. It is interesting that near Cœtivy Island, turbulent processes reach maximal activity in the middle water layers. Exchange coefficients at a depth of 30 m are 3 times greater than at 10 m in depth. The pulse-rate intensity at the edge of a coral plateau (African Banks, $J_{v,u} = 0.82-1.20$) and in the subsurface layer over a reef slope (Cœtivy, $J_{v,u} = 0.97 - 1.06$) exceeds values at the water surface

(Cöetivy, $J_{v,u} = 0.47-0.57$).

Water motion over island platforms showed less activity. Thus, the windward western coast of Cöetivy Island is bathed by a north/northeasterly current (Fig. 5, St. 1), with mean speeds of $10-25 \text{ cm}\cdot\text{sec}^{-1}$ and maximal values ($32-38 \text{ cm}\cdot\text{sec}^{-1}$) observed both at the surface and at the lower layer of the current. In the bottom layer, the current changes direction to southeast and its speed does not exceed $4 \text{ cm}\cdot\text{sec}^{-1}$.

Tidal variability of currents (Fig. 5, St. 3) increases at coastal promontories of the island where currents can change direction from northwest to southeast at mean speeds of $20-26 \text{ cm}\cdot\text{sec}^{-1}$. Horizontal turbulent exchange in the surface layer (10 m) over the western reef flat of Cöetivy Island is almost 3 times less than for the same depth in waters of the eastern coast. In the middle layers this difference increases and becomes 6-fold greater (Table 2). Exchange coefficients range from 10^3 to $10^6 \text{ cm}^2\cdot\text{sec}^{-1}$, but immediately over the bottom of the reef platform they decrease to $10^2-10^3 \text{ cm}^2\cdot\text{sec}^{-1}$, with the current becoming more unstable ($J_{v,u} = 1.23 - 1.39$). Near the bottom, turbulent processes within the zone of coastal coral communities (5-8 m) exceed turbulent levels at the boundary of coral distribution, on average, by 300 times and show maximal variability because of bottom roughness.

In cases where island plateaus on relic lagoon bases, as happens near the northwestern coast of Desroches Island, circulation around the island shows slower current speeds. Near the northwestern coast of the island, water motion reverses with the current direction changing from southwestern to north-eastern at mean speeds of $2-5 \text{ cm}\cdot\text{sec}^{-1}$ and maximal ones at $22-25 \text{ cm}\cdot\text{sec}^{-1}$ (Table 2, St. 7). Near the bottom, the current turns toward the east and southeast and becomes more stable with mean speeds of to $6-14 \text{ cm}\cdot\text{sec}^{-1}$. Periodic wave currents with high speeds appear on coastal shallows with gentle bottom slopes during storm conditions as, for example, the current of up to $50 \text{ cm}\cdot\text{sec}^{-1}$ that was recorded over a *Thalassia* meadow near the northwestern coast of Desroches Island at a depth of 4.5 m during a period of northwesterly winds (Table 1, St. 8). Also a very weak current ($2-4 \text{ cm}\cdot\text{sec}^{-1}$) running northeastward (Table 2, St. 9) is present near the opposite leeward (southeastern) coast, separated by a reef crest. Currents over the sunken lagoon have high pulse capacities ($J_{v,u} = 6.27$ to 6.57) demonstrated by a variable range of coefficients of turbulent exchange ($10^4-10^5 \text{ cm}^2\cdot\text{sec}^{-1}$). Near the bottom, turbulent exchange decreases ($A_{\text{max}} = 10^3-10^4 \text{ cm}^2\cdot\text{sec}^{-1}$), whereas maximal coefficients of turbulent exchange were observed near the northwest coast of the island, in the zone of wave-induced currents ($A_{\text{max}} = 10^5-10^6 \text{ cm}^2\cdot\text{sec}^{-1}$). Near the leeward southeastern coast, turbulence was weak with the orientation of maximal turbulent exchange being both longitudinal and nearly diametrically opposed to the direction of the dominating current. The degree of anisotropy of turbulent exchange increases with decreasing distance to the coast.

Turbulent vortices in the coastal zones of calcareous islands are caused mainly by tidal processes with periods of 12-24 h (Fig. 6). The effect of hydrodynamic processes on a large synoptical scale (average recording period of 48 h or more) is not as pronounced. Tidal cycles (with fluctuation periods of 3.5-4, 12 and 16 h) play the most important role in the structure of turbulent fluctuations observed in a given current. Additionally, functions of spectral density of speed pulsation reveal the presence of large vortices with periods of 16-18, 27-28 and 30-35 h as well as orographic and wave pulsations of a given current (periods of 1-3 h).

Thermohaline conditions, hydrochemical and optical features.

Analysis of data from the reef flat on the western coast of Cöetivy Island showed an absence of significant temperature stratification. Wind and wave action caused mixing of warm and less saline surface waters (temperature greater than 27.5°C , salinity less than 34.9 ppt) down to 15-25 m in

depth (Fig. 8 A, B, St. 1). Deeper, there were colder (25-26°C) and more saline (greater than 34.95 ppt) waters. Near the western coast of the island, surface water temperatures increased from 27.54 to 28.10°C. Some decrease in salinity was observed due to precipitation. Vertical temperature variability was influenced little by tidal processes.

The eastern slope of Cœtivy Island was much more affected by hydrological processes of the open sea. For example, on 16 January 1989, at the reef crest, an intensive input of cooler and more saline waters characteristic of the south subtropical intermediate water mass was observed (minimal temperature 15.4°C, salinity 35.21 ppt), which probably was caused by upwelling of deep waters due to strong (up to 25 m·sec⁻¹) westerly winds and tidal processes (Fig. 9 A, B, St. 2). The same phenomena resulted in a 4.19°C temperature difference between the surface and a depth of 10 m at a station 300 m off the leeward eastern coast. The temperature gradient between surface and deep waters was 2-2.5°C per 10 m. On the whole, waters of the eastern coast were cooler and more saline than those of the western coast.

Oxygen concentrations near the eastern coast of Cœtivy Island conform well to the temperature patterns described above. During the entire period of study, the oxygen concentrations at the surface exceeded 100% saturation. The minimal value (60.5%) correlated with an influx of cooler waters found at a depth of 44 m (Fig. 9 C). Near the western coast of Cœtivy (Fig. 8 C, St. 1) an oxygen deficiency was observed which shifted towards the surface layers during the night (up to 92.3% saturation at 1.3 m in depth). The minimal oxygen concentration (77%) was found near the bottom (30 m) at 300 hrs local time on 13 January 1989.

Values of pH near Cœtivy Island were 8.27-8.32 but towards the coast they decreased to 8.06. However, in warm intertidal pools, rich in all nitrogen forms as well as phosphates, pH reached values of 8.75-9.02.

Penetration of cool subsurface waters into shallow areas was recorded near Cerf Island (Providence, 19.6 m depth), as well as near Cœtivy Island. The difference between near-surface (28.45°C) and near-bottom temperatures was 4.4°C. The presence of upwelling of transformed deep waters is also confirmed by a sharp drop (to 87.5% saturation) of oxygen concentration in near-bottom waters. Salinities seaward of Cerf Island ranged from 34.76-34.83 ppt. At the surface near the coast, salinity varied from 34.6 to 34.7 ppt, temperature - from 28.3 to 29.8°C and near the bottom from 34.5 to 34.7 ppt and from 27.9 to 28.1°C. pH varied slightly (from 8.2 to 8.28).

The coastal area of South Island (African Banks) was homogeneous in thermohaline features up to the boundary of the reef plateau (16 m depth). During a 24 h survey, seawater temperatures ranged between 27.9-28.1°C and salinity varied between 35.12 to 35.48 ppt. Oxygen concentrations were 100-107% saturated and the pH varied from 8.22 to 8.29.

Transformed equatorial subsurface waters found along the northwestern shallows of Desroches Island showed highly homogeneous temperatures (27.4-28.9°C) and salinities (34.88-34.99 ppt). Variability of thermohaline indices was slight in seaward and coastal areas, which suggest an efficient water exchange. The amplitude of the 24 h temperature range near the water surface was 1.5°C (from 28.6 to 30.1°C), near the bottom - 0.5°C (from 27.6 to 28.2°C), while the salinity deviated only 0.07 ppt over the entire water column and the pH ranged from 8.3 to 8.4.

Near Cœtivy Island, the optical boundary of the change in water type is at approximately 6 m in depth. In the upper layers, K is 0.115, which corresponds to coastal type I water. Deeper than 6 m, there is a layer corresponding to ocean type I water (K= 0.057). Near Providence, the optical types of water masses were similar to those of Cœtivy: the surface water layer (6 m deep) corresponded to coastal type I water (K= 0.135) and deeper there were clearer waters of the ocean type I (K=

0.047). Off the coast of African Banks, the optical type changed at a depth of than 1.8 m with waters of coastal type III ($K= 0.168$) below and waters of coastal type IX ($K= 0.791$). Around Desroches Island, the optical type of waters changed at the 3 m depth where the less saline and more turbid upper surface layer corresponded to the coastal type V ($K= 0.250$) and waters of ocean type III were observed deeper than 3 m.

This study did not reveal consistent differences in concentrations of nutrients for islands of different origin, i.e., coral vs. granitic (Table 3), since both types had habitats of both low and high enrichment (e.g., upwelling, birds, sewage). The greatest range of diurnal and spatial variability of nutrients was found near Cœtivy Island where waters were rich in phosphates and silic acid, 0.4 and $3.74 \mu\text{g}\cdot\text{atom}\cdot\text{l}^{-1}$, respectively. The highest concentrations were observed in intertidal and upper subtidal zones and especially in warmed intertidal pools where high concentrations of all forms of nutrients (phosphorus, nitrogen, silicon) were found. The pH values reached 9.0 which suggests high levels of production processes. The greatest biomass of macrobenthos (especially of *Thalassodendron ciliatum*, reported by Gutnik et al., Ch. 5 this issue) was also found in the intertidal zone of Cœtivy.

The source of phosphates in the coastal waters of Cœtivy Island is partly to an influx of deep waters rich in nutrients, which was observed both at the eastern dropoff or along the shallow western coasts (Table 4).

The coastal waters of Cerf Island (Providence Group) are notable for their high levels of nitrates and organic nitrogen: $0.59\text{-}0.88$ and $16.8\text{-}17.5 \mu\text{g}\cdot\text{atom}\cdot\text{l}^{-1}$, respectively (Table 3). Higher concentrations of phosphates and nitrates in surface waters were observed near the reef crest on the southeastern side of the island, and reached $0.25\text{-}0.27$ and $0.83\text{-}1.16 \mu\text{g}\cdot\text{atom}\cdot\text{l}^{-1}$, respectively. Additionally, in shallow waters 300-500 m offshore, at a depth of 0.7-2.5 m, the phosphate concentration also increased.

The coastal surface waters of South Island (African Banks) have low mean levels of phosphates and silicon: 0.14 and $1.37 \mu\text{g}\cdot\text{atom}\cdot\text{l}^{-1}$, respectively (Table 3). In shallow waters, higher concentrations of organic phosphorus were found, and highest levels for African Banks occurred in immediate proximity to the coast: $0.29\text{-}0.21 \mu\text{g}\cdot\text{atom}\cdot\text{l}^{-1}$. Concentrations of silicon, ammonia, nitrates and organic nitrogen did not change as a function of the distance from the shore and nitrites were absent.

According to the 24 h survey southeast of African Banks, the concentrations of phosphates, silicon and nitrates in the surface waters and near the bottom did not change substantially throughout the day and ranged from $0.08\text{-}0.18$, $1.2\text{-}2.55$ and $0.02\text{-}0.08 \mu\text{g}\cdot\text{atom}\cdot\text{l}^{-1}$, respectively. An inverse relationship was observed in the 24 h variation of organic phosphorus and nitrogen concentrations.

The concentrations of nutrients in the coastal waters of Desroches, both on the windward and leeward sides, were similar in mean values to those for the other islands studied. The 24 h variation of nutrients in the lagoon area at 0, 10 and 25 m depths showed maximal variability at the 10 m depth. At this level, 24 h variations of inorganic and organic phosphorus ranged from 0.16 to 0.54 and 0.02 to $0.39 \mu\text{g}\cdot\text{atom}\cdot\text{l}^{-1}$, respectively, changing in inverse relation but without apparent regularity. Phosphorus and silicon concentrations in both surface and bottom waters were stable and did not change over time. The 24 h observations of nutrients were carried out at windward and leeward island sites 150-200 m offshore. Silicic acid concentrations in coastal waters varied from 2.05 to $4.45 \mu\text{g}\cdot\text{atom}\cdot\text{l}^{-1}$. Phosphorus values (both organic and inorganic) were similar at both stations and corresponded to the photosynthetic pattern, with minimal PO_4 -levels recorded at 2000 hrs, at the highest oxygen concentration. During the night, phosphate concentrations increased,

probably due to the destruction of organic phosphorus, which was in inverse concentration to that of phosphates. The fluctuation of PO_4 -concentrations was somewhat greater ($0.11\text{-}0.61 \mu\text{g-atom}\cdot\text{l}^{-1}$) while that of nitrates was smaller ($0\text{-}0.77 \mu\text{g-atom}\cdot\text{l}^{-1}$) on the leeward side than on the windward side. These differences are likely to be the result of higher current speeds on the windward side and more active mixing and water exchange between the submerged lagoon and open ocean waters. In contrast, to the less dynamic coastal waters of the southeastern side are protected by the island and reef from wind and wave action.

Atolls (Farquhar, St. Joseph, Cosmoledo, Aldabra and Astove)

Atoll islands are widely distributed in the Indian Ocean. Farquhar, St. Joseph, Cosmoledo, Astove and Aldabra have shallow lagoons connected with the open ocean by one or several channels. Oceanic process affect only the outer slopes of the atolls whereas hydrological conditions in the lagoons separated from the ocean by land or by the reef platform mainly depend on tides cycles, winds, evaporation and precipitation.

The outer reef slope of the eastern coast of Farquhar Atoll is washed by a strong ($50\text{-}70 \text{ cm}\cdot\text{sec}^{-1}$) northeasterly current. Mean current speeds of St. Joseph's southeastern coast range between $24\text{-}36 \text{ cm}\cdot\text{sec}^{-1}$ (Fig. 10, St. 15). Near Wizard Island (Cosmoledo Atoll), the southwesterly current speed was $17\text{-}31 \text{ cm}\cdot\text{sec}^{-1}$ (Fig. 11, St. 18). Typical current speeds near the eastern coast of Aldabra Atoll were $15\text{-}30 \text{ cm}\cdot\text{sec}^{-1}$. Localized turbulent vortices and tidal fluctuations caused short term increases in current speeds of $1 \text{ m}\cdot\text{sec}^{-1}$ or more in all areas under study.

Near the bottom, current speeds decreased considerably. For example, rough coral substrata near Farquhar Atoll at 18 m in depth reduced the current speed to $2\text{-}4 \text{ cm}\cdot\text{sec}^{-1}$ (St. 6). In the narrow channel between D'Arros Island and the western coast of St. Joseph Island, the speed of a reverse current near the base of a coastal coral-dominated reef ranged between 2 and $9 \text{ cm}\cdot\text{sec}^{-1}$ (Fig. 10, St. 16). The reef crest is characterized by increased hydrodynamic activity. On the southeast coast of Cosmoledo Atoll, the reef is characterized by higher water exchange due to an offshore current coming onto the reef platform and dividing into many differently directed flows with speeds of around $25\text{-}35 \text{ cm}\cdot\text{sec}^{-1}$. Closer to the coast, the dissipation of water motion energy continues. Maximal current speeds in the study areas of Farquhar and St. Joseph reef-flats did not exceed $14 \text{ cm}\cdot\text{sec}^{-1}$ (St. 5 and 17).

Coefficients of horizontal turbulent exchange over outer atolls slopes were in the order of 10^4 to $10^7 \text{ cm}^2\cdot\text{sec}$, decreasing with an increase in protection from wave action (Farquhar - 1.1×10^6 , Cosmoledo - 1.3×10^5 , St. Joseph - 8.9×10^4 , Aldabra - $3.8 \times 10^4 \text{ cm}^2\cdot\text{sec}^{-1}$). Pulsation patterns of currents depend on their inherent stability. On outer atoll reef slopes in deep water with stable currents, the turbulence is usually less than on shallow reef platforms.

The greatest current speeds in atoll lagoons can be observed in direct proximity to channels which provide lagoons with water influx and outflux during each tidal cycle. Observations made in the large lagoon of Cosmoledo Atoll revealed the presence of strong tidal currents with mean speeds of $2\text{-}15 \text{ cm}\cdot\text{sec}^{-1}$ (strongest currents of $24\text{-}27 \text{ cm}\cdot\text{sec}^{-1}$) which provide active mixing ($A_{\text{max}} = 1.7 \times 10^4 \text{ cm}^2\cdot\text{sec}^{-1}$). At the same time, in some lagoon sites separated by temporary barriers and shallows, water currents tend to be weak. This phenomenon promotes the accumulation of fine-grained sediments. One such example is the western side of St. Joseph Atoll, where current speeds did not exceed $2\text{-}4 \text{ cm}\cdot\text{sec}^{-1}$ and the average value of coefficients of horizontal turbulent exchange was $8 \times 10^2 \text{ cm}^2\cdot\text{sec}^{-1}$ (Fig. 10, St. 17). The influx of turbulent kinetic energy ceases for values of averaging periods from 2 to 24 h (Fig. 12), suggesting that the main processes causing instability of the water column near atoll coasts are tides, winds and wave currents. Anisotropy of turbulent exchange is

most distinctly displayed in areas of stable current action. The direction of maximal turbulent exchange to a large degree coincides with the current direction in cases of strong current.

Distribution functions in the spectral density of kinetic energy due to turbulent pulsations in current speeds reveal a 12 h period as a main peak of energy supply (Fig. 13). Farther offshore, additional sources of large scale current pulsations are vortices with 14-18 h periods (resonance or orographic). Tidal modes of smaller periods (6-7 or 3-4 h) and currents of wind-wave origin (1-2 h) can be found at shallow depths. Inside the lagoon of St. Joseph Atoll, the main effect on hydrodynamics is probably produced by wind action with a period of 24-25 h, and in the lagoon at Cosmoledo 30-35 h fluctuations related to weather conditions were observed.

Thermohaline conditions, optical and hydrochemical features.

Lagoons produce a substantial effect on the physical-chemical characteristics of coastal waters of atolls. Lagoons are regions in which waters coming in from the open ocean become transformed, depending on the degree of isolation and meteorological conditions. Thus, in the rainy period of 22 January 1989, at the northeastern part of Farquhar Atoll's lagoon, the salinity did not exceed 33.85 ppt at a depth of 0.8 m, and during the stable sunny weather of 12 March 1989, salinity reached 36.3 ppt at the surface in the central part of the lagoon, while near the bottom (5 m depth) it was 38.66 ppt. On the whole, the temperature and salinity of surface waters ranged from 26.2-27.6°C and 34.77-35.04 ppt, respectively.

At low tide, lagoon waters penetrate into the outer boundary waters of atolls and alter their thermohaline structure. Thus, active turbulence near atoll coasts causes mixing of warm lagoon waters to greater depths levels and the appearance of temperature inversions (Fig. 14, St. 4), e.g., at 10 m in depth the temperature was 27.3°C while at 30 m in depth it was 27.6°C. Near the bottom (45-50 m), an influx of cool (23-24°C) surface south subtropical waters was observed. Stronger winds causes an increase of the temperature gradient ($1.4^{\circ}\text{C}\cdot\text{m}^{-1}$) in the contact zone between different water masses.

During the daytime, a reduced level of dissolved oxygen was observed around Farquhar at 15-25 m in depth. In the second half of the day, the boundary of 100% oxygen saturation was lowered to the 50 m level. Maximal oxygen concentrations coincided with the period of maximal intensity of photosynthesis, while pH values ranged between 8.42-9.38.

Near Astove, thermohaline characteristics changed from the channel to the lagoon. In the shallow lagoon at 1 m in depth, the salinity was 35.1 ppt and temperature 32.3°C; in the surface layer of the lagoon area of the channel, salinity was 35.5° ppt and temperature was 35.2°C; in the seaward part of the channel - 35.2 ppt and 31.4°C; and at 2.5 km westwards from the channel - 34.7 ppt and 29.2°C. The high photosynthetic intensity during the daytime caused a considerable oxygen oversaturation of lagoon waters of up to 132%.

Active water mixing near Cosmoledo Atoll resulted in lagoon temperature fluctuations from 29.1 to 30.6°C, and salinity changes from 34.5 to 34.8 ppt while in outer coastal zone, temperatures ranged from 29.0 to 29.2°C and the salinity was 34.9 ppt. Oxygen saturation levels of waters at Station 18 (Cosmoledo Atoll) ranged from 101-103% saturation down to a depth of 20 m. The pH ranged between 8.3-8.4. Similar to findings near Cosmoledo, a high degree of homogeneity (salinity= 35 ppt) was observed in the surface lagoon waters and outer reef slope waters of St. Joseph Atoll. The range of temperature fluctuations at the surface was 0.4°C (from 27.8 to 28.2°C) and near the bottom 0.3°C (from 27.6 to 27.9°C). Salinity at the surface ranged from 35.24 to 35.46 ppt, near the bottom it was 35.45 ppt. Oxygen saturation levels of surface waters were 104-106% and

100-102% near bottom. The pH varied between 8.2 and 8.4.

The most characteristic features of vertical thermohaline structure of waters near South Island (Aldabra Atoll) were cyclic temperature and salinity patterns in near bottom waters with a fluctuation period of about 12 h and amplitude of 4°C (23.5-27.5°C). The upwelling of cooled subsurface waters corresponded to low tide waters and downwelling occurred during high water. Fluctuations became appreciable below 20 m in depth. Shallower there was a homogeneous temperature layer (27.7-27.9°C) with a salinity of 34.94 to 34.99 ppt. The influx of cooled waters was caused by upwelling from the upper zone of intermediate south subtropical waters. Their deepwater origin is indicated by both a salinity increase (up to 35.08 ppt) with a sharp drop in oxygen concentration (down to 85% saturation) in the bottom layer, while oxygen saturation at the surface was 108-110%.

The optical characteristics of the various atolls studied displayed vertical differences. For example, the subsurface waters of Farquhar Atoll related to the ocean type II ($K= 0.098$) down to 6 m in depth, near Aldabra Atoll, the surface layer to 3 m was occupied by waters of coastal type VII ($K= 0.462$), and at Cosmoledo Atoll surface waters were coastal type I ($K= 0.138$) down to 8.2 m in depth. In these regions, bottom waters were ocean type I ($K= 0.047-0.052$). St. Joseph and Astove Atolls were similar to ocean optical type III subsurface waters ($K= 0.101-0.106$). The 7 m surface near Astove corresponded to the coastal type III ($K= 0.189$) and at St. Joseph the surface layer was the coastal type V ($K= 0.256$) to 1 m in depth.

The lagoon waters of these atolls, as a rule, had unique hydrochemical features in comparison with waters surrounding their atolls as well as between each other in terms of chemical composition and productivity. High concentrations of inorganic phosphorus, silicon and organic nitrogen were observed in Farquhar Lagoon, where the highest productivity of phytoplankton occurred (communication of V. M. Gol'd), an influx of deep oceanic waters enriched with phosphates was observed here during maximal low waters near the southeastern coast of the atoll at 50 m in depth (Table 5).

High concentrations of organic phosphorus were found in the coastal and lagoon waters of Cosmoledo Atoll ($0.74-0.85 \mu\text{g}\cdot\text{atom}\cdot\text{l}^{-1}$) and Astove Atoll ($0.29-0.73 \mu\text{g}\cdot\text{atom}\cdot\text{l}^{-1}$), which are obviously related to the great number of nesting colonies of birds at these islands. Astove Atoll has a submerged shore line with a steep slope which provides quick dispersion of organic phosphorus in deep waters and, as a result, a considerable difference between concentrations of organic phosphorus in the lagoon versus the surrounding waters. Organic nitrogen concentrations were also high but varied considerably ($8-17 \mu\text{g}\cdot\text{atom}\cdot\text{l}^{-1}$). High concentrations of nitrates ($0.5-0.9 \mu\text{g}\cdot\text{atom}\cdot\text{l}^{-1}$) and ammonia were found only in the surface layers (Cosmoledo - $0.36-0.90 \mu\text{g}\cdot\text{atom}\cdot\text{l}^{-1}$; Astove - $0.94-1.63 \mu\text{g}\cdot\text{atom}\cdot\text{l}^{-1}$) and suggest a high rate of transformation of organic nitrogen of birds excreta into other nitrogen forms. Similarly, high levels of nitrates ($1 \mu\text{g}\cdot\text{atom}\cdot\text{l}^{-1}$) and organic nitrogen ($15-17 \mu\text{g}\cdot\text{atom}\cdot\text{l}^{-1}$) in the coastal and lagoon waters of Aldabra, without a simultaneous increase in phosphorus concentrations, may be the result of activities of nitrogen-fixing microorganisms.

It is known that tidal exchanges can lead to nutrient enrichment of lagoon waters from oceanic sources, filling the lagoon during high tide and creating conditions for increases in primary productivity. During low tide, waters depauperate in inorganic elements leave the lagoon. Silicon concentrations in Aldabra Lagoon followed this pattern; during high tide silicon increased from 1.75 to $2.1-2.5 \mu\text{g}\cdot\text{atom}\cdot\text{l}^{-1}$ and dropped at low tide. This relationship was not found for other nutrients (Table 6).

At the same time, 24 h observations in the channel to Farquhar Lagoon showed that during low tide the outer side of the atoll was enriched with nutrients running out of the lagoon, whereas during

high tide, oceanic surface waters poor in nutrients entered the lagoon (Table 7).

It is obvious that oligotrophic oceanic water masses surrounding tropical reefs ultimately eliminate differences in nutrient supply between islands of different origins i.e., calcareous or granitic. Lagoon waters retain an individuality which depends both on the exchange processes with the ocean expressed during tidal cycles and on complex biotic conditions in the lagoons and on atoll coasts. Intertidal waters, as a rule, tend to show increased levels of nutrients due to the production activities of biotas confined at shallow depths.

CONCLUSIONS

1. The geomorphological complexity of the islands investigated greatly affects oceanographic processes in their immediate vicinity.

2. Regions of the outer reef slopes are the most hydrodynamically active. Current speeds in these habitats can reach tens of centimeters per second, and separate short-term flow pulses can exceed $1 \text{ m}\cdot\text{sec}^{-1}$. The most intensive processes of turbulent exchange ($A_{\text{max}} = 10^4\text{-}10^7 \text{ cm}^2\cdot\text{sec}^{-1}$) also occur here. Reef platforms with typically rugose reliefs reduce current speeds both in the water column and near the bottom. Mean current speeds in subsurface layers of outer reef slopes are $30\text{-}40 \text{ cm}\cdot\text{sec}^{-1}$ ($A_{\text{max}} = 10^3\text{-}10^4 \text{ cm}^2\cdot\text{sec}^{-1}$), and near the bottom currents seldom exceed $5\text{-}10 \text{ cm}\cdot\text{sec}^{-1}$ ($A_{\text{max}} = 10^2\text{-}10^3 \text{ cm}^2\cdot\text{sec}^{-1}$).

Coastal wave currents with speeds up to $50 \text{ cm}\cdot\text{sec}^{-1}$ and exchange processes in the range of $10^5\text{-}10^6 \text{ cm}^2\cdot\text{sec}^{-1}$ may appear here (e.g., Desroches). In contrast, typical current speeds for coastal shallows protected from wind and waves are $2\text{-}4 \text{ cm}\cdot\text{sec}^{-1}$ ($A_{\text{max}} = 10^2\text{-}10^5 \text{ cm}^2\cdot\text{sec}^{-1}$). Narrowing of channels, which appears in the sedimentary locations of reefs and banks near Mahé Island and St. Joseph Atoll, promotes an increase of water exchange over the reef slope, with current speeds being $20\text{-}30 \text{ cm}\cdot\text{sec}^{-1}$ ($A_{\text{max}} = 10^4\text{-}10^6 \text{ cm}^2\cdot\text{sec}^{-1}$). Water movement in atoll lagoons depends on the proximity of channels exchanging of water during a tidal cycle. In sites having the most intensive flows, mean current speeds may reach $15\text{-}20 \text{ cm}\cdot\text{sec}^{-1}$ ($A_{\text{max}} = 10^3\text{-}10^5 \text{ cm}^2\cdot\text{sec}^{-1}$), however, lagoons subjected to intensive sedimentation are characterized by weak currents with $2\text{-}5 \text{ cm}\cdot\text{sec}^{-1}$ speed ($A_{\text{max}} = 10^2 \text{ cm}^2\cdot\text{sec}^{-1}$).

3. The main causes of turbulence on reefs are periodic processes with typical periods from 2 to 12-24 h. This is most conspicuous during tidal cycles with 12 and 6 h periods. Near the larger islands (e.g., Mahé) and also in St. Joseph and Cosmoledo Atoll lagoons, the turbulent effects of winds (24 h period) can be observed. Vortices, presumably of orographic or resonance origin, have periods of 16-18 h, large scale weather fluctuations of 30-40 h are also found in atoll lagoons. High frequency current pulses (1-3 h) can be observed in almost all portions of a reef profile and are related to wind and wave effects.

4. In the Seychelles region, three water masses were distinguished: surface equatorial, surface south subtropical and intermediate south subtropical. The islands investigated can be conditionally subdivided into two groups: northern (Mahé, La Digue, Praslin, Desroches) and southern (Astove, Providence, Aldabra, Cosmoledo, Farquhar, Cœtivy). The salinity of the water mass surrounding the northern group remains lower than 35.04 ppt. Such differentiation of surface waters is correlated with the location of the south tropical frontal water boundary.

5. Hydrological conditions in coastal island waters with fringing and platform reefs (Mahé, La Digue, Praslin, African Banks, Desroches, Cœtivy) depend to a large extent on hydrological processes of the surrounding ocean waters. Waters overlying reef platforms have more uniform

thermohaline characteristics. On island slopes (Cœtivy, Cerf, Aldabra, Farquhar), upwelling of cold subsurface waters resulted in differences between surface and near bottom temperatures of 4-12°C in coastal areas. The influx of subsurface waters had a cyclic nature and its intensity depended on interactions between storm wind drift and tidal rhythm.

6. The nutrient study showed concentrations in the coastal zones of the Seychelles that are similar to coral reef areas. In the coastal zones, phosphate concentrations are somewhat higher than in the open ocean, and the amount of organic phosphorus is close to that of inorganic phosphorus if there is no additional influx of P-PO₄ from greater depth (Cœtivy, Providence), sewage input from land (Mahé) or organic phosphorus from excrement of birds inhabiting some of the islands (Astove, Cosmoledo). On the whole, as occurs on other tropical reefs, the quantity of nutrients in Seychelles waters is not great, with the presence of semi-enclosed nutrient exchanges accounting for much of the productivity of their ecosystems.

REFERENCES

- Anon. 1979. Methods of chemical analysis in hydrobiological research. Vladivostok. 132 pp.
- Atkinson, M. 1981. Phosphate flux as a measure of the net coral reef flat productivity. Pages 417-418, in Proc. 4th Int. Coral Reef Symp., Manila, Vol. 1.
- Bishev, V.I., B.G. Kort and I.G. Usychenko. 1977. Probability structure of the currents in the equator region of the Indian Ocean. Pages 91-103, in Collection: Hydrology of the Indian Ocean. Moscow.
- Brown, B.E. and R.P. Dunne. 1980. Environmental controls of patch-reef growth and development. Mar. Biol. 56 (1):85-96.
- Burkov, V.A. and V.G. Neiman. 1977. General circulation of waters of the Indian Ocean. Pages 3-90, in Hydrology of the Indian Ocean. Moscow, Science Publishers.
- Burkov, V.A. 1982. Peculiarities of hydrology. Pages 63-86, in Geography of the World Ocean. Indian Ocean. Science Publishers, Leningrad.
- Ertel, H. 1932. Allgemeine Theorie der Turbulenzreibung des Austausches Sitzungen. Ber. Preuss. Acad. Wiss. Math. Phys. Kl. V. 26.
- Frith C.A. (nee Ludington). 1981. Circulation in a platform reef lagoon, One Tree Reef, Southern Great Barrier reef. Pages 347-353, in Proc. 4th Int. Coral Reef Symp., Manila, Vol. 1.
- Gallagher, B.S., K.M. Shimada, F.J. Gonzalez and E.D. Stroup. 1971. Tides and currents in Fanning Atoll lagoon. Pac. Sci. 25(2):191-205.
- Gusev, A.M., L.K. Moiseev and A.I. Nemytov. 1980. Coastal wind circulation around islands and atolls. Pages 198-218, in Papers of the Institute of Oceanology, Academy of Sciences of the USSR, Vol. 90.
- Hamner, W.M. and I.K. Hauri. 1981. Effects of island mass: Water flow and plankton patterns around a reef in GBR lagoon, Australia. Limnol Oceanogr 26(6):1084-1102.

- Hatcher, A.J. and B.G. Hatcher. 1981. Seasonal and spatial variation in dissolved inorganic nitrogen in the One Tree Reef lagoon. Pages 419-424, in Proc. 4th Int. Coral Reef Symp., Manila, Vol. 1.
- Jerlov, N.G. 1980. Sea optics. Hydro-meteorological Publishers, Leningrad. 248 pp.
- Konnov, V.A. and A.D. Scherbinin. 1975. Distribution of nutrients and water exchange of coral island lagoons with surrounding ocean areas. Pages 171-174, in Chemical oceanography of investigation of seas and oceans. Science Publishers, Moscow.
- Kwei, E.A. 1977. Biological, chemical and hydrological characters of coastal lagoons Ghana, West Africa. *Hydrobiol.* 56(2):157-174.
- Magnier, J. and B. Wanthy. 1976. Esquisse hydrologique du lagoon de Tokopoto (Tuamotou). Pages 279-287, in Can. ORSTOM Oceanogr. Vol. 14(4).
- Marsac, F., B. Piton, M. Potier and B. Stequert. 1983. Campagne expérimentale de pêche à la senne du thonier "Yves de Kerguelen" dans l'ouest de l'Océan Indien tropical. Mission ORSTOM Seychelles, Rapp. Scient. Nr 5. 98 pp.
- Marsac, F. and J.P. Hallier. 1985. Environment et pêche thonière de surface dans l'Océan Indien occidental (1983-1984). Mission ORSTOM Seychelles, Rapp. Scient. Nr 5. 98 pp.
- Mergner, H. and H. Schuhmacher. 1974. Morphologie, Ökologie und Lon'erung von Korallonriffen Bei Agaba (Golf von Agaba, Rotes Meer). *Helgol. Meeresunters.* 26:238-258.
- Morozov, E.G., E.A. Plahin and A.S. Samodurov. 1977. To the problem of generation of short-period internal waves. Pages 136-139, in Hydrology of the Indian Ocean. Science Publishers, Moscow.
- Munk, W.H. and M.C. Sargent. 1954. Adjustment of Bikini Atoll to ocean waves. U. S. Geol. Surv. Prof. Paper. 260(C):275-280.
- Murray, S.P. and H.H. Roberts. 1977. Nearshore current fields around coral islands control on sediment accumulation and reef growth. Pages 54-59, in Proc. 3rd Int. Coral Reef Symp.
- Ozmidov, R.V. 1968. Horizontal turbulence and turbulent exchange in the ocean. Science Publishers, Moscow. 196 pp.
- Potier, M. and F. Marsac. 1984. La pêche thonière dans l'Océan Indien: campagne exploratoire d'un flottille de senneurs (1982-1983). Mission ORSTOM Seychelles, Rapp. Scient. Nr 4. 73 pp.
- Roberts, H.H., S.P. Murray and J.N. Suhayda. 1977. Physical processes in a fore-reef shelf environment. Pages 507-515, in Proc. 3rd Int. Coral Reef Symp.
- Roberts, H.H. and J.N. Suhayda. 1977. Wave and current interactions on a fringing coral reef crest Great Corn Island, Nicaragua. Pages 161-162, in GUA Pap. Geol., Ser. 1 Nr 9.
- Roberts, H.H., J.M. Murray, S.P. and D.K. Hubbard. 1981. Offshelf sediment transport on the downdrift of a Trade wind island. Pages 389-397, in Proc. 4th Int. Coral Reef Symp., Manila, Vol. 1.

- Shtockmann, V.B. 1940. About turbulent exchanges in the middle and south part of the Caspian Sea. Pages 269-292, in Papers of the Academy of Sciences of the USSR. Geography and geophysics, Nr 4.
- Smith, S.V. 1983. Net production of coral reef ecosystems. Pages 127-131, in The ecology of deep and shallow coral reefs. NOAA Symp. Ser. for Undersea Res. Vol. 1(1).
- Sorokin, Y.I. 1977. Productivity of marine communities. Page 224, in Ocean Biology. Biological productivity of the ocean. Moscow.
- Sorokin, Y.I. 1986. Problems of productivity, trophology and energetic balance of coral reef ecosystems. Mar. Biol. (Vladivostok) 6:3-14.
- Strickland, J.D.H. and T.R. Parsons. 1972. A manual of seawater analysis (2nd edition). Bull. Fish. Res. Board Can. 38 (1):1-310.
- Storr, I.F. 1964. Ecology and oceanography of the coral reef tract Abaco Island, Bahamas. Geol. Soc. Amer. Spec. Paper. Nr 79. 98 pp.
- Stroup, E.D. and G.A. Mayers. 1974. The flood-tide jet in Fanning island lagoon. Pac. Sci. 28 (3):211-223.
- Suhayda, I.N. and H.H. Roberts. 1977. Wave action and sediment transport of fringing reefs. Pages 65-70, in Proc. 3th Int. Coral Reef Symp.
- Von Arx, W.S. 1948. The circulation systems of Bikini and Rongelap lagoons. Trans. Amer. Geophys. Union. Vol. 29:861-871.
- Walderrama, I.C. 1981. Determination of total form phosphorus and nitrogen. J. Mar. Chem. 10:109-122.
- Wolanski, E. 1981. Aspects of physical oceanography of the Great Barrier Reef lagoon. Pages 375-381, in Proc. 4th Int. Coral Reef Symp., Manila, Vol. 1.
- Wolanski, E. and G.L. Pickard. 1983. Upwelling by internal tides and Kelvin waves at the continental shelf on the GBR. Aust. J. Mar. Freshw. Res. 34:65-80.

Table 1. Characteristics of hydrological stations.

Station	Location	Coordinates	Date	Period of Observation	Horizon	Weather Condition
1	Cöetivy	= 7° 8.3' = 56° 15.2'	13-15/1/89	49	10	NW, W wind 4-25 m·sec ⁻¹
1	Cöetivy	= 7° 8.3' = 56° 15.2'	13-14/1/89	28	20	NW, W wind 6-10 m·sec ⁻¹
1	Cöetivy	= 7° 8.3' = 56° 15.2'	14-15/1/89	32	28.5	NW, W wind 4-25 m·sec ⁻¹
2	Cöetivy	= 7° 9' = 56° 17.9'	15-17/1/89	34	10	NW, W wind 3-13 m·sec ⁻¹
2	Cöetivy	= 7° 9' = 56° 17.9'	15-17/1/89	34	30	NW, W wind 3-13 m·sec ⁻¹
3	Cöetivy	= 7° 12' = 56° 11.3'	14-15/1/89	18	4.5	NW, W wind 1-10 m·sec ⁻¹
4	Farquhar	= 10° 11.2' = 51° 11.3'	20-23/1/89	68	20	NW, W wind 5-12 m·sec ⁻¹
5	Farquhar	= 10° 8.8' = 51° 11.6'	21-23/1/89	55	8.5	NW, W wind 6-8 m·sec ⁻¹
6	Farquhar	= 10° 8.9' = 51° 11.8'	21-22/1/89	29	17.5	NW, W wind 5-8 m·sec ⁻¹
7	Desroches	= 5° 40.4' = 53° 39.3'	6-10/2/89	102	20	NW, W, N wind 2-14 m·sec ⁻¹
7	Desroches	= 5° 40.4' = 53° 39.3'	6-8/2/89	58	24.5	NW, W, N wind 3-14 m·sec ⁻¹
8	Desroches	= 5° 41.7' = 53° 40.1'	7-8/2/89	17	4.5	NW, W wind 3-14 m·sec ⁻¹
9	Desroches	= 5° 41.2' = 56° 39.8'	9-10/2/89	21	4.5	NW wind 3-8 m·sec ⁻¹
10	Praslin	= 4° 22.6' = 55° 44.2'	11-13/2/89	45	15	calm, NW, W wind 2-4 m·sec ⁻¹
11	Praslin	= 4° 21.4' = 55° 45.8'	11-13/2/89	46	9.5	calm, NW, W wind 2-4 m·sec ⁻¹

Table 1. Continued.

Station	Location	Coordinates	Date	Period of Observation	Horizon	Weather Condition
12	Mahé	= 4° 36.36' =55° 28.5'	15-24/2/89	206	9.5	NW, W wind 2-8 m·sec ⁻¹
13	Mahé	= 4° 37.42' =55° 29.22'	15-20/2/89	118	3.5	NW, W wind 2-8 m·sec ⁻¹
14	African	= 4° 55.9' =53° 23.6'	27-28/2/89	24	16	NW wind 2-5 m·sec ⁻¹
15	St. Joseph	= 5° 27.7' =53° 23.6'	2-4/3/89	49	15	NW, N wind 2-7 m·sec ⁻¹
16	St. Joseph	= 5° 24.64' =53° 19.04'	1-4/3/89	71	26.5	NW, N wind 2-7 m·sec ⁻¹
17	St. Joseph	= 5° 24.92' =53° 19.35'	1-4/3/89	68	2.5	NW, N wind 2-7 m·sec ⁻¹
18	Cosmoledo	= 9° 44.9' =47° 39.5'	7-9/3/89	43	12	E, NE wind 2-15 m·sec ⁻¹
19	Cosmoledo	= 9° 44.9' =47° 39.5'	7-9/3/89	50	11.5	E, NE wind 2-15 m·sec ⁻¹
20	Cosmoledo	= 9° 43.62' =47° 37.23'	7-9/3/89	57	2.5	E, NE wind 2-15 m·sec ⁻¹
21	Aldabra	= 9° 25' =46° 32'	27-28/2/89	30	20	N, NW wind 2-5 m·sec ⁻¹

Table 2. Current parameters and characteristics of horizontal turbulent exchange in the studied areas. y/W_y = current direction (in degrees) / density of direction probability. V/W_v = current speed ($\text{cm}\cdot\text{sec}^{-1}$) / density of rate probability. $J_{u,v}$ = mean turbulent intensity for speed vector components. α = direction of maximal turbulent exchange, in degrees. $\epsilon = A_{\max}/A_{\min}$ - index of anisotropy of turbulent exchange.

Station	Horizon, m	y/W_y	V/W_v	J_v	J_u	A_{\max}	α	ϵ
1	10	<u>25-30</u> 0.02 <u>55-60</u> 0.01	<u>10-14</u> 0.05 <u>15-19</u> 0.04	0.35 ± 0.26	0.39 ± 0.27	$177\cdot 10^3\pm$ $14\cdot 10^3$	57	9.9
1	20	<u>50-54</u> 0.02	<u>15-24</u> 0.01	0.48 ± 0.35	0.51 ± 0.35	$225\cdot 10^3\pm$ $25\cdot 10^3$	59	9.5
1	28.5	<u>135-140</u> 0.01	<u>2-4</u> 0.2	1.39 ± 0.74	1.23 ± 0.78	$2\cdot 10^3\pm$ $0.2\cdot 10^3$	85	7.7
2	10	<u>30-40</u> 0.02	<u>2-4</u> 0.05 <u>15-19</u> 0.02	0.51 ± 0.37	0.47 ± 0.36	$500\cdot 10^3\pm$ $81\cdot 10^3$	70	7.0
2	30	<u>35-50</u> 0.02	<u>25-30</u> 0.02	0.94 ± 0.31	0.89 ± 0.24	$903\cdot 10^3\pm$ $533\cdot 10^3$	75	10.0
3	4.5	<u>285-295</u> .01-.02	<u>15-19</u> 0.02	2.57 ± 1.94	1.71 ± 0.77	$604\cdot 10^3\pm$ $168\cdot 10^3$	84	22.7
4	20	<u>15-20</u> 0.02 <u>195-200</u> 0.02	<u>25-30</u> 0.02 <u>40-50</u> 0.02 <u>60-65</u> 0.01	0.78 ± 0.52	0.69 ± 0.48	$1154\cdot 10^3\pm$ $101\cdot 10^3$	71	5.6
5	8.5	<u>340-350</u> 0.01	<u>2-9</u> .06-.09	1.07 ± 0.76	0.88 ± 0.94	$27\cdot 10^3\pm$ $4\cdot 10^3$	84	4.6
6	17.5	<u>20-30</u> 0.02 <u>200-215</u> 0.014	<u>2-4</u> 0.004	1.29 ± 0.89	1.07 ± 1.33	$15\cdot 10^3\pm$ $0.6\cdot 10^3$	91	8.7
7	20	<u>50-55</u> 0.08 <u>245-250</u> 0.08	<u>10-15</u> 0.004	6.57 ± 11.68	6.27 ± 7.77	$11\cdot 10^3\pm$ $4.6\cdot 10^3$	76	11.4
7	24.5	<u>125-129</u> 0.01	<u>2-4</u> 0.13	1.29 ± 0.89	0.82 ± 0.61	$8\cdot 10^3\pm$ $1.1\cdot 10^3$	103	9.4

Table 2. Continued

Station	Horizon, m	y/W_y	V/W_v	J_v	J_u	A_{max}	α	ϵ
8	4.5	<u>80-90</u> 0.06 <u>145-150</u> 0.01	<u>20-24</u> 0.07	1.66 ± 1.21	1.19 ± 0.72	$504 \cdot 10^3 \pm$ $105 \cdot 10^3$	81	7.7
9	4.5	<u>45-50</u> 0.03	<u>2-4</u> 0.2	0.12 ± 0.22	0.48 ± 1.79	$31 \cdot 10^3 \pm$ $26 \cdot 10^3$	54	397.4
10	15	<u>100-110</u> 0.01 <u>300-305</u> 0.08	<u>10-14</u> 0.04 <u>20-24</u> 0.05	36 ± 0.26	0.50 ± 0.34	$120 \cdot 10^3 \pm$ $15 \cdot 10^3$	121	7.7
11	9.5	<u>300-304</u> 0.08	<u>2-4</u> 0.2	9.40 ± 4.99	8.5 ± 3.1	$3 \cdot 10^3 \pm$ $0.3 \cdot 10^3$	91	5.5
12	9.5	<u>270-275</u> .01-.02	<u>15-19</u> 0.1	1.35 ± 1.10	1.13 ± 0.84	$199 \cdot 10^3 \pm$ $10 \cdot 10^3$	116	7.0
13	3.5	<u>60-80</u> .015-.016	<u>15-20</u> 0.06	0.42 ± 0.36	0.50 ± 0.29	$161 \cdot 10^3 \pm$ $11 \cdot 10^3$	54	6.5
14	16	<u>95-100</u> 0.02	<u>15-19</u> 0.04 <u>25-30</u> 0.03	1.20 ± 0.53	0.82 ± 0.45	$407 \cdot 10^3 \pm$ $61 \cdot 10^3$	83	9.1
15	15	<u>55-65</u> 0.011 <u>215-220</u> 0.010	<u>20-24</u> 0.03 <u>40-45</u> 0.03	0.51 ± 0.27	0.58 ± 0.24	$89 \cdot 10^3 \pm$ $10 \cdot 10^3$	79	5.8
16	26.5	<u>5-15</u> 0.03 <u>195-200</u> 0.02	<u>2-4</u> 0.10 <u>10-15</u> 0.02	0.31 ± 0.24	0.70 ± 0.58	$10 \cdot 10^3 \pm$ $3 \cdot 10^3$	65	17.9
17	2.5	<u>275-280</u> 0.02 <u>330-335</u> 0.02	<u>2-4</u> 0.17	0.15 ± 0.26	0.10 ± 0.11	$0.8 \cdot 10^3 \pm$ $0.3 \cdot 10^3$	60	20.4
18	12	<u>75-80</u> 0.006 <u>205-210</u> 0.01	<u>5-10</u> 0.04 <u>30-34</u> 0.04	0.74 ± 0.38	0.67 ± 0.36	$126 \cdot 10^3 \pm$ $17 \cdot 10^3$	80	9.6

Table 2. Continued

Station	Horizon, m	y/W_y	V/W_v	J_v	J_u	A_{max}	α	ϵ
19	11.5	$\frac{175-180}{0.01}$ $\frac{215-220}{0.01}$	$\frac{20-29}{0.10}$	1.29 ± 0.58	1.13 ± 0.68	$286 \cdot 10^3 \pm 32 \cdot 10^3$	104	6.1
20	2.5	$\frac{5-9}{0.02}$ $\frac{180-195}{0.03}$	$\frac{5-10}{0.06}$	0.43 ± 0.27	1.04 ± 0.76	$17 \cdot 10^3 \pm 4 \cdot 10^3$	57	15.5
21	20	$\frac{350-355}{0.02}$	$\frac{2-4}{0.15}$ $\frac{55-70}{0.03}$	0.22 ± 0.31	0.20 ± 0.36	$38 \cdot 10^3 \pm 1.3 \cdot 10^3$	64	10.2

Table 3. Concentration of nutrients in surface waters of the Seychelles Islands (January - March, 1989). n = number of samples taken.

Island	n	$\mu\text{g-atom}\cdot\text{l}^{-1}$			n	$\mu\text{g-atom}\cdot\text{l}^{-1}$			
		phosphate	organic phosphorus	silicon		nitrites	ammonia	nitrates	organic nitrogen
Cœtivy									
coastal	10	0.46±0.21	0.15±0.12	3.74±1.32	6	0.32±0.13	1.09±1.06	3.35±4.10	28.48±20.8
ocean	6	0.25±0.05	0.12±0.11	2.90±0.26	2	0-0.34	0-0.42	0-0.48	7.1-13.1
Farquhar									
coastal	3	0.27±0.09	0.23±30.17	2.42±0.79	2	0.13±0.14	0.05±0.07	0.1±0.14	7.45±3.61
ocean	4	0.22±0.04	0.13±0.04	2.29±0.16	1	0.17	0	1.2	-
lagoon	3	0.36±0.18	0.06±0.07	3.23±0.25	3	0.10±0.02	1.43±0.67	1.6±0.85	26.5±2.33±
Aldabra									
coastal	3	0.21±0.04	0.22±0.06	2.16±0.39	3	0.05±0.16	0.54±0.16	1.36±0.25	18.37±2.22
ocean	4	0.20±0.07	0.16±0.04	2.08±0.19	1	0	0	0.11	15.9
lagoon	6	0.20±0.03	0.12±0.04	1.91±0.36	3	0.02±0.03	0.30±0.12	1.26±0.18	16.67±3.71
Desroches									
coastal lagoon	6	0.24±0.11	0.11±0.04	2.49±0.37	4	0.08±0.02	0.63±0.48	0.6±0.66	14.13±1.91
coastal ocean	6	0.25±0.13	0.12±0.09	2.79±0.87	5	0.03±0.04	0	0.35±0.32	13.36±2.54
central lagoon	7	0.20±0.07	0.17±0.07	2.30±0.12	1	0.04	0.02	0.11	7.5
African Banks									
coastal	3	0.14±0.06	0.32±0.04	1.37±0.08	3	0	1.07±0.92	0.11±0.05	10.3±4.97
ocean	5	0.14±0.05	0.19±0.11	1.70±0.48	5	0.76±1.70	0.76±1.70	0.09±0.05	7.6±3.1
St. Joseph									
coastal	5	0.14±0.06	0.16±0.05	1.5±0.19	5	0	0.48±0.53	0.78±0.19	8.83±0.29
ocean	5	0.17±0.06	0.18±0.07	1.79±0.19	5	0	0.41±0.54	0.52±0.04	10.78±3.7
lagoon	2	0.09±0.04	0.33±0.12	1.68±0.04	2	0	0.5	0.76±0.09	7.8±2.12
Providence									
coastal	4	0.24±0.04	0.21±0.04	1.90±0.06	4	0	0.17±0.22	0.59±0.16	16.83±4.9
ocean	2	0.21±0.08	0.23±0.13	2.44±0.06	2	0	0	0.88±0.40	17.45±1.7
Cosmoledo									
coastal	1	0.21	1.48	2.15	2	0.27±0.38	0.27±0.38	0.44±0.02	9.5±4.95
ocean	4	0.13±0.03	0.85±0.77	2.16±0.26	4	0	0.27±0.14	0.45±0.04	17.63±6.5
lagoon	7	0.25±0.17	0.81±0.26	2.34±0.26	7	0	0.33±0.40	0.57±0.18	17.28±2.8

Table 3. Continued

Island	n	phosphate	organic phosphorus	silicon	n	nitrites	ammonia	nitrates	organic nitrogen
Astove coastal	1	0.23	0.16	1.8	1	0	0.94	0.95	-
ocean	3	0.20±0.05	0.29±0.13	2.20±0.65	3	0	0.41±0.81	0.58±0.25	9.17±1.21
lagoon	2	0.13±0.04	0.73±0.05	1.21±0.79	2	0	0.73±0.77	0.44±0.02	8.3±2.55
Mahé coastal	9	0.24±0.09	0.11±0.06	2.31±0.53	6	0.09±0.05	0.52±0.79	0.21±0.23	12.12±6.6
Praslin coastal	3	0.10±0.03	0.2±0.01	2.11±0.42	1	0	3.1	0.3	8.4
ocean	4	0.14±0.02	0.2±0.03	2.30±0.2	2	0	0-1.0	0.0-0.6	11.22-15.1
La Digue coastal	3	0.17±0.08	0.15±0.1	2.05±0.14	4	0	0.19±0.24	0.25±0.2	8.97±3.56
ocean	1	0.08	0.16	1.97	1	0	0	0.0	11.9

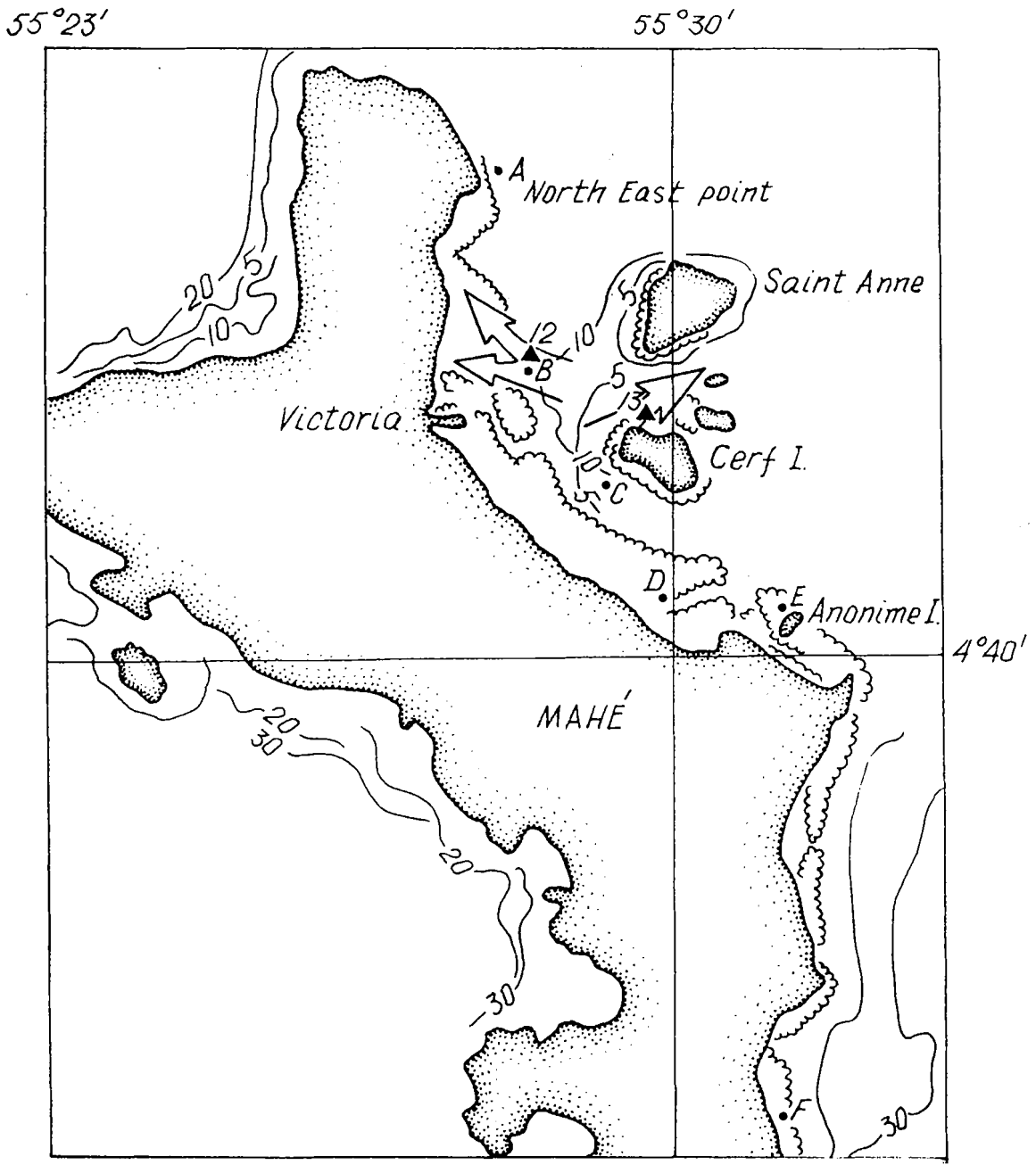


Figure 1. Scheme of hydrological stations at Mahé.

Designations:

- ↖ - subsurface currents
- ↖ - near-bottom currents
- - stations with full complex of hydrological observations
- * - stations of underwater light measurements
- - hydrochemical sections
- ▲ - stations of near-bottom current measurements

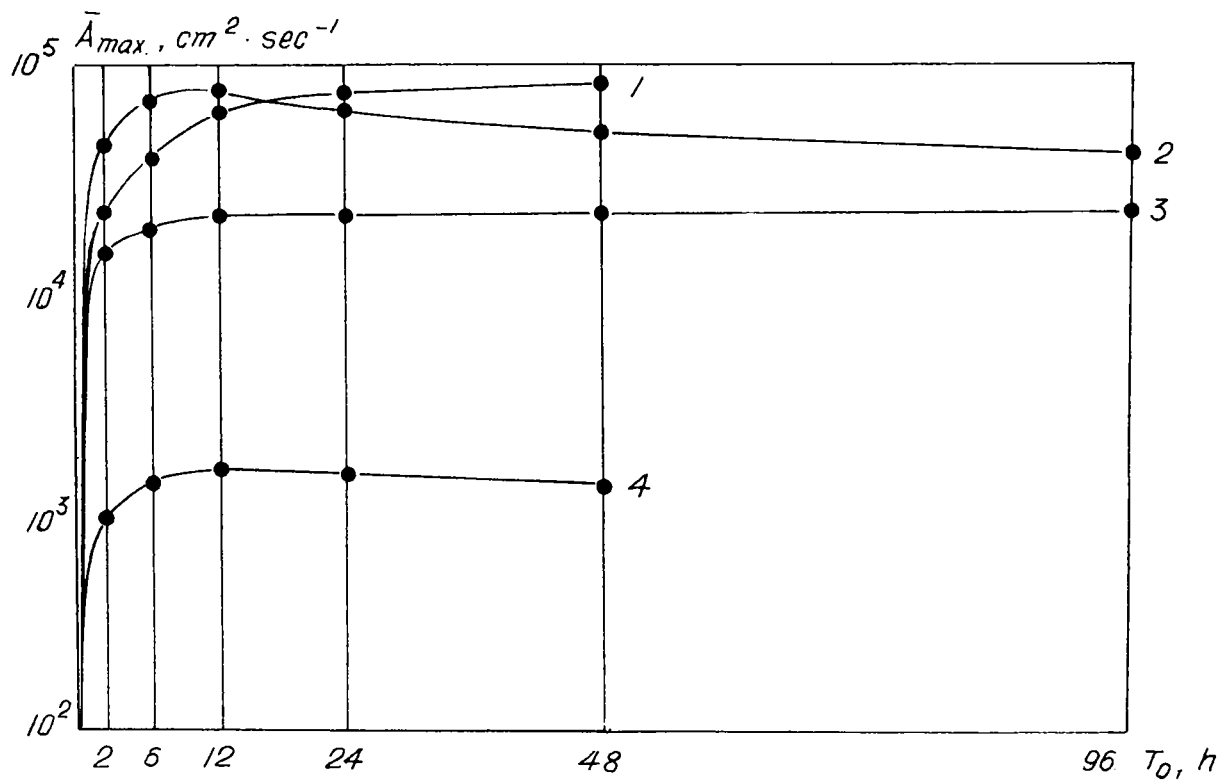


Figure 2. Change of mean maximal coefficients of horizontal turbulent exchange of motion quantity (\bar{A}_{max}) with the increase of averaging period (T_0) at granite islands:

- 1 - south coast of Praslin, station 10, horizon 15 m, depth of 23 m.
- 2 - northeastern coast of Mahé, anchorage in port, station 12, horizon 9.5 m, depth of 10 m.
- 3 - northeastern coast of Mahé, station 13, horizon 3.5m, depth of 4 m.
- 4 - south coast of Praslin, station 11, horizon 9.5 m, depth of 10 m.

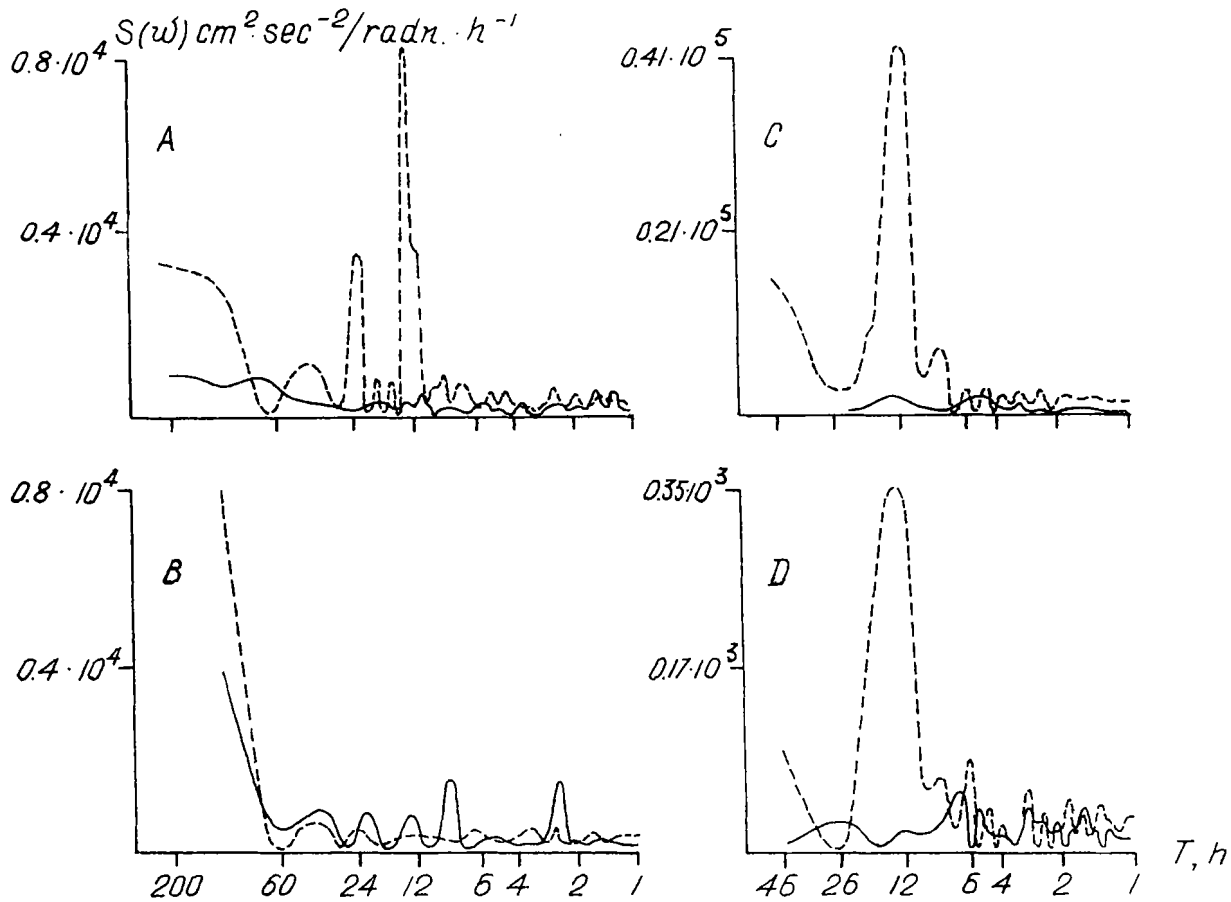


Figure 3. Functions of spectral density of current rate pulse at granitic islands:

A - northeastern coast of Mahé, anchorage in the port, station 12, horizon 9.5 m, depth 10 m.

B - northeastern coast of Mahé, shallow at the Cerf Is., horizon 3.5 m, depth of 4 m.

C - south coast of Praslin, station 10, horizon 15 m, depth of 23 m.

D - south coast of Praslin, station 11, horizon 9.5 m, depth of 10 m.

Continuous line shows the function for meridional component of current speed vector, interrupted one - for a zonal component.

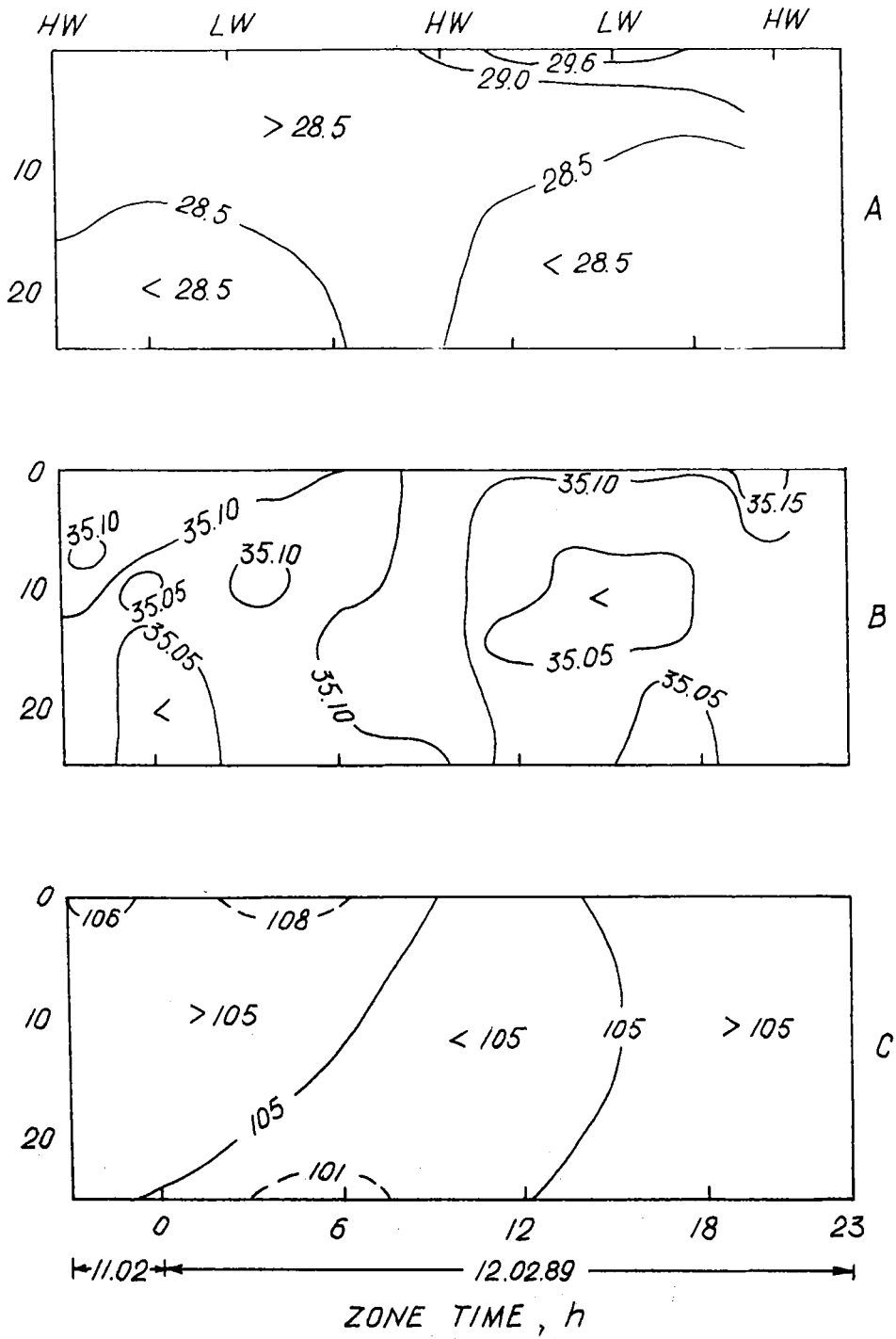


Figure 4. Fluctuations of temperature (A), salinity (B) and dissolved oxygen concentration (C) at Praslin.

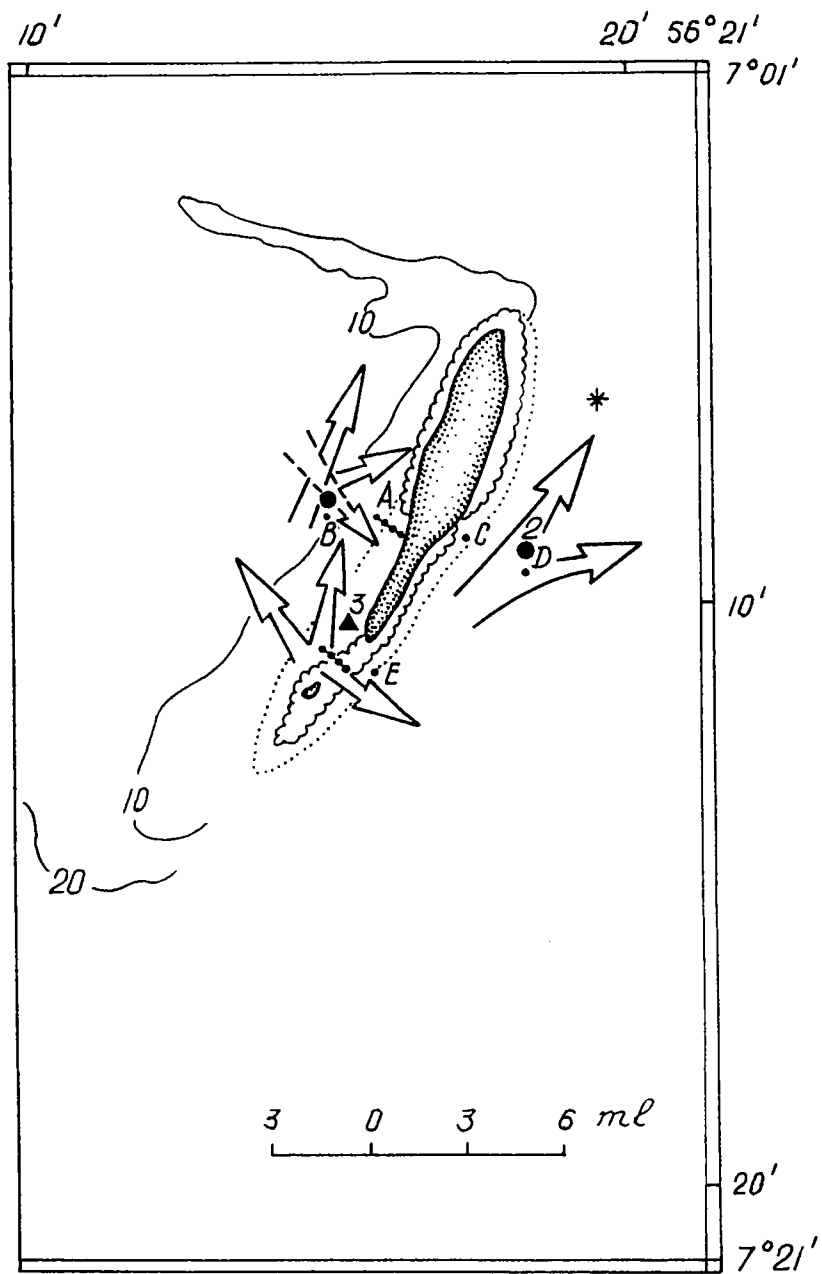


Figure 5. Scheme of hydrological stations and currents at Cöetivy.

Designations:

- ↗ - subsurface currents
- ↘ - near-bottom currents
- - stations with full complex of hydrological observations
- * - stations of underwater light measurements
- - hydrochemical sections
- ▲ - stations of near-bottom current measurements

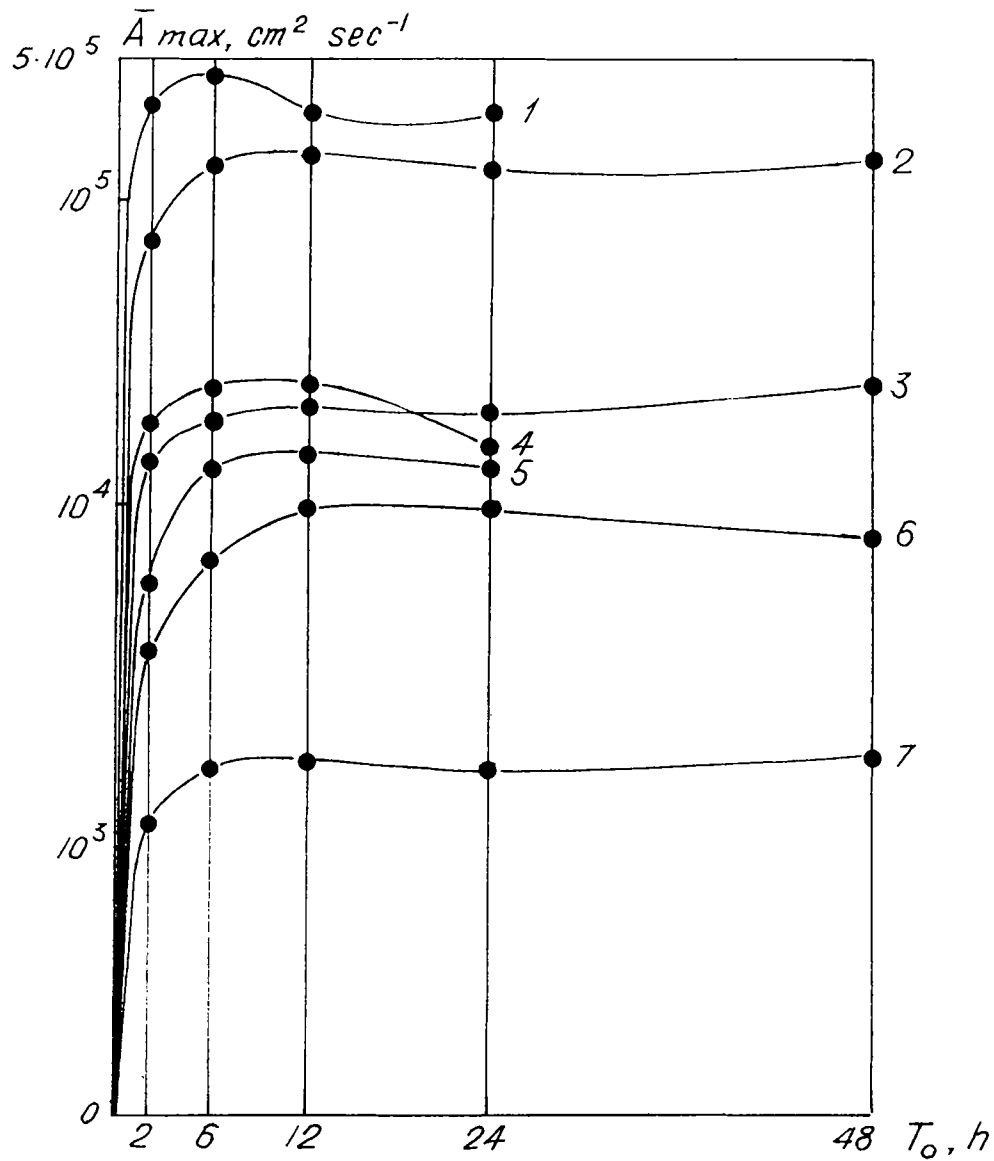


Figure 6. Fluctuations of averaged maximal coefficients of horizontal turbulent exchange of motion quantity (A_{max}) caused by the increase of averaging period (T_o) at Cöetivy.

- 1 - northwestern coast, station 8, horizon 4.5 m, depth of 5 m.
- 2 - eastern coast, station 2, horizon 30 m, depth of 50 m.
- 3 - eastern coast, station 2, horizon 10 m, depth of 50 m.
- 4 - western coast, station 3, horizon 4.5 m, depth of 5 m.
- 5 - western coast, station 1, horizon 4.5 m, depth of 29 m.
- 6 - western coast, station 1, horizon 10 m, depth of 29 m.
- 7 - western coast, station 1, horizon 8.5 m, depth of 29 m.

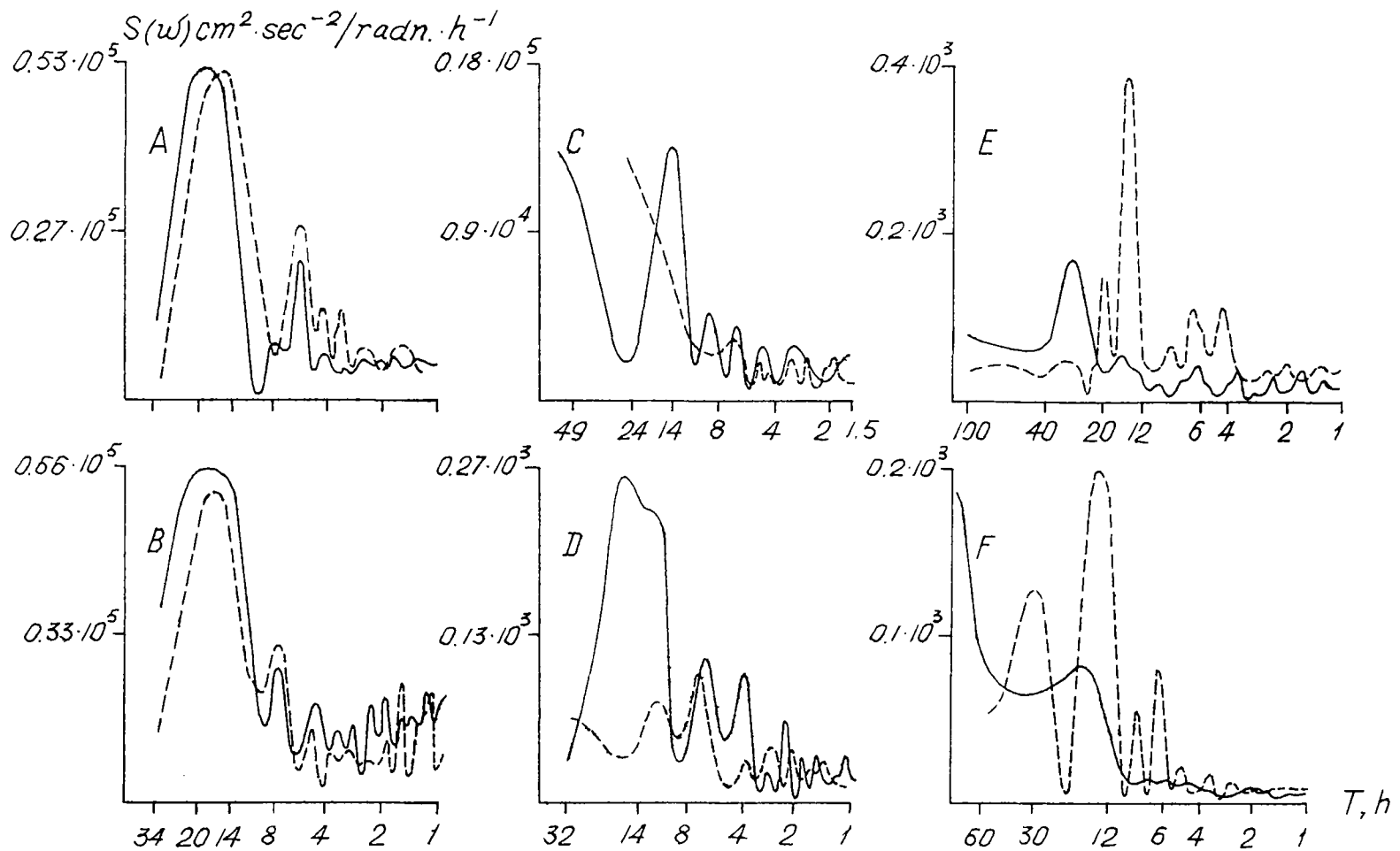


Figure 7. Functions of spectral density of current rate pulse at coral islands.

- A - Cöetivy, east coast, station 2, horizon 10 m, depth of 50 m.
- B - Cöetivy, east coast, station 2, horizon 30 m, depth of 50 m.
- C - Cöetivy, west coast, station 1, horizon 10 m, depth of 29 m.
- D - Cöetivy, west coast, station 1, horizon 28.5 m, depth of 29 m.
- E - Desroches, northwestern coast, station 7, horizon 20 m, depth of 25 m.
- F - Desroches, northwestern coast, station 7, horizon 24.5 m, depth of 25 m.

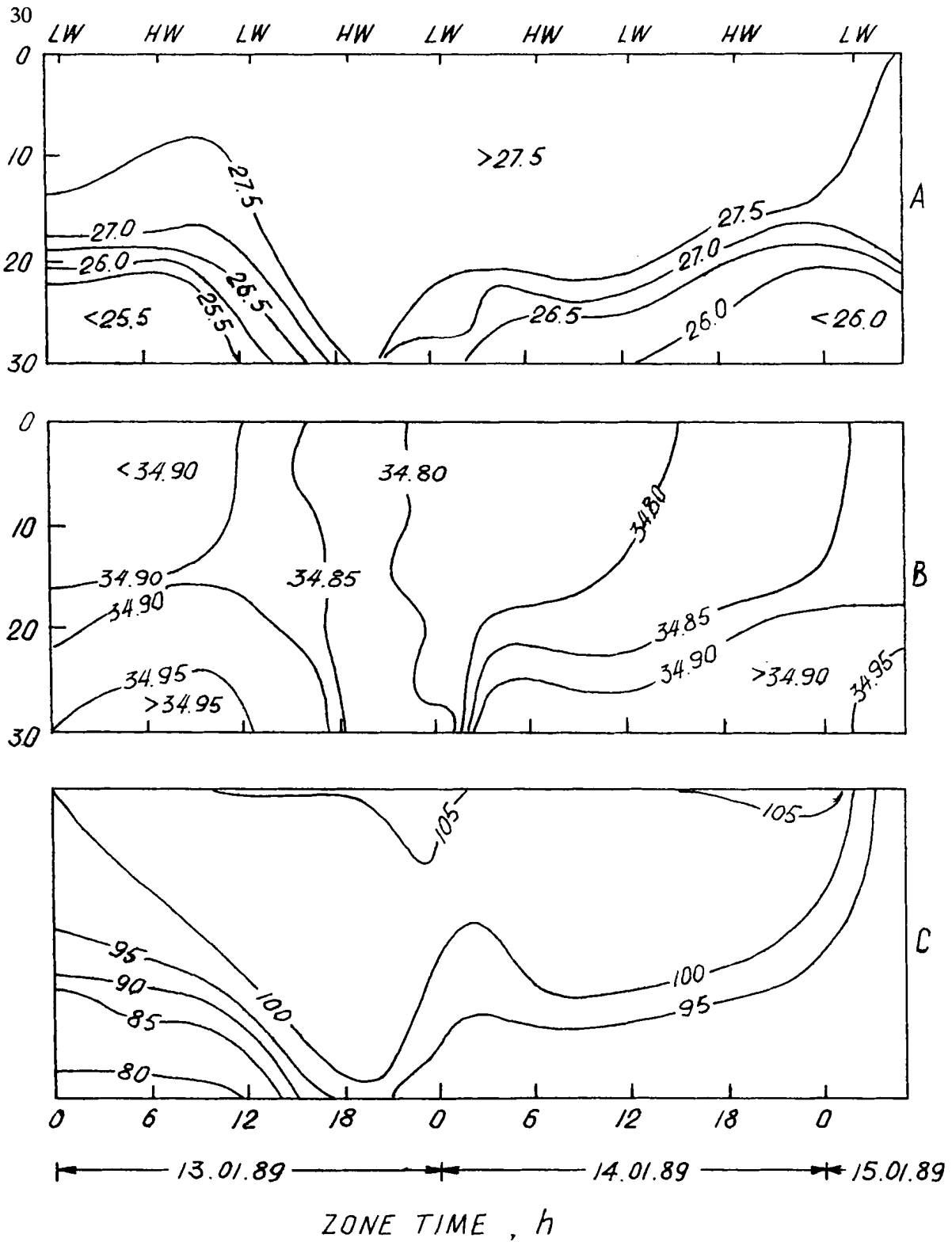


Figure 8. Temporal variability of temperature (A), salinity (B) and dissolved oxygen concentration (C) at Station 1, Cöetivy.

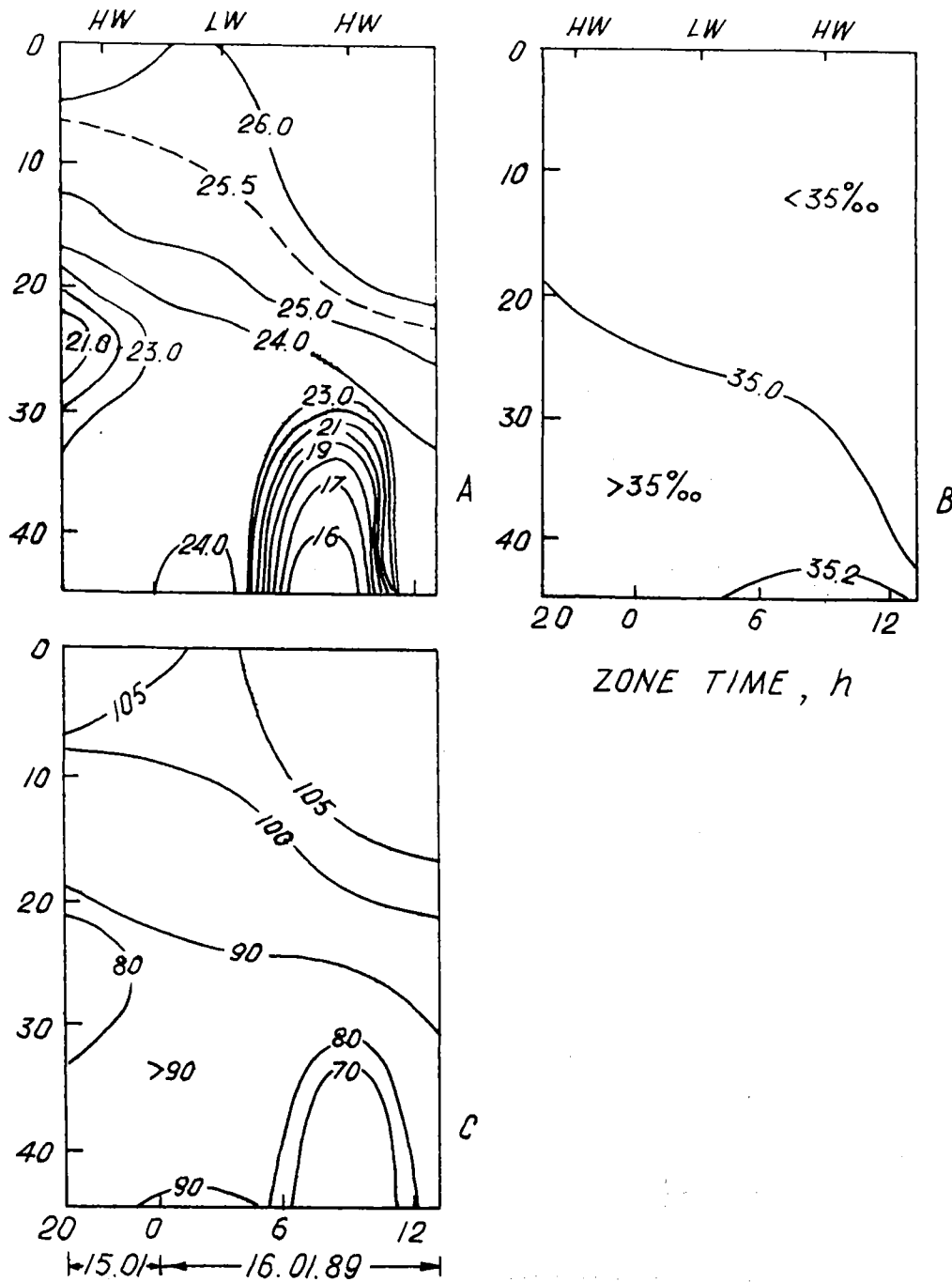


Figure 9. Temporal variability of temperature (A), salinity (B) and dissolved oxygen concentration (C) at Station 2, Coetivy.

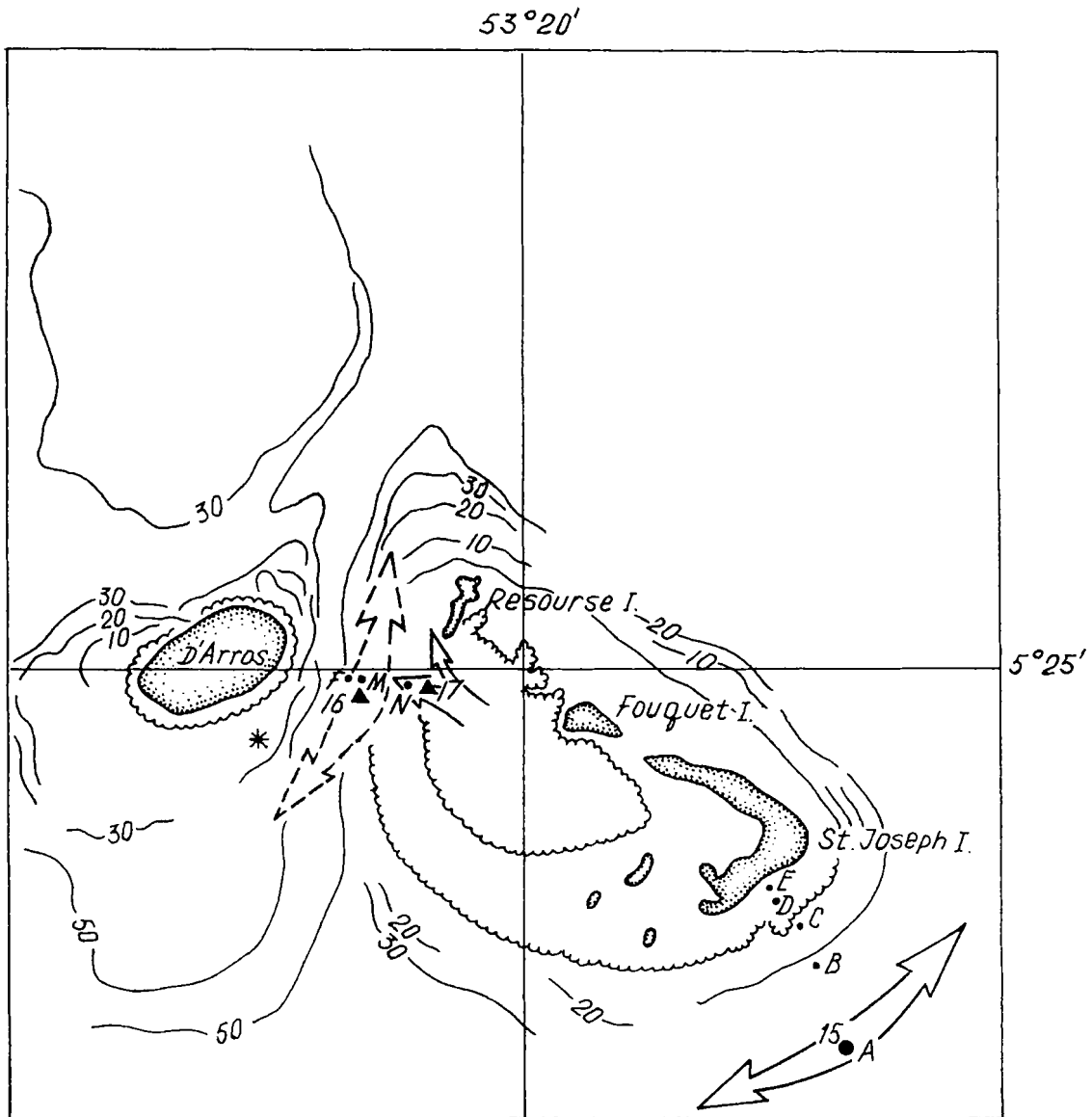
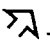
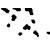






Figure 10. Scheme of hydrological stations and currents at western (A) and eastern (B) coasts of St. Joseph.

Designations:

-  - subsurface currents
-  - near-bottom currents
-  - stations with full complex of hydrological observations
-  - stations of underwater light measurements
-  - hydrochemical sections
-  - stations of near-bottom current measurements

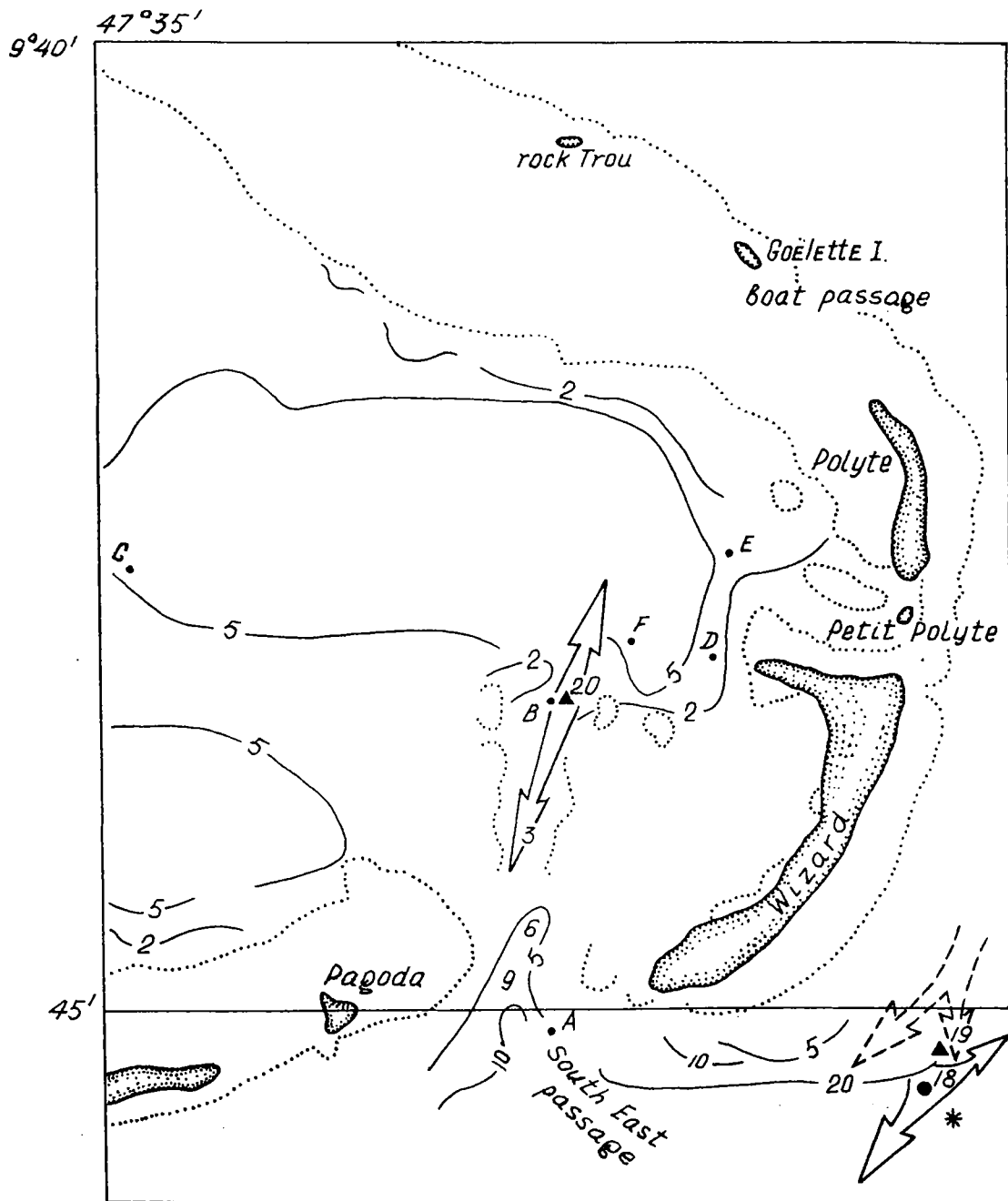


Figure 11. Scheme of hydrological stations and currents at southeastern coast of Cosmoledo.

Designations:

- ↗ - subsurface currents
- ↘ - near-bottom currents
- - stations with full complex of hydrological observations
- * - stations of underwater light measurements
- - hydrochemical sections
- ▲ - stations of near-bottom current measurements

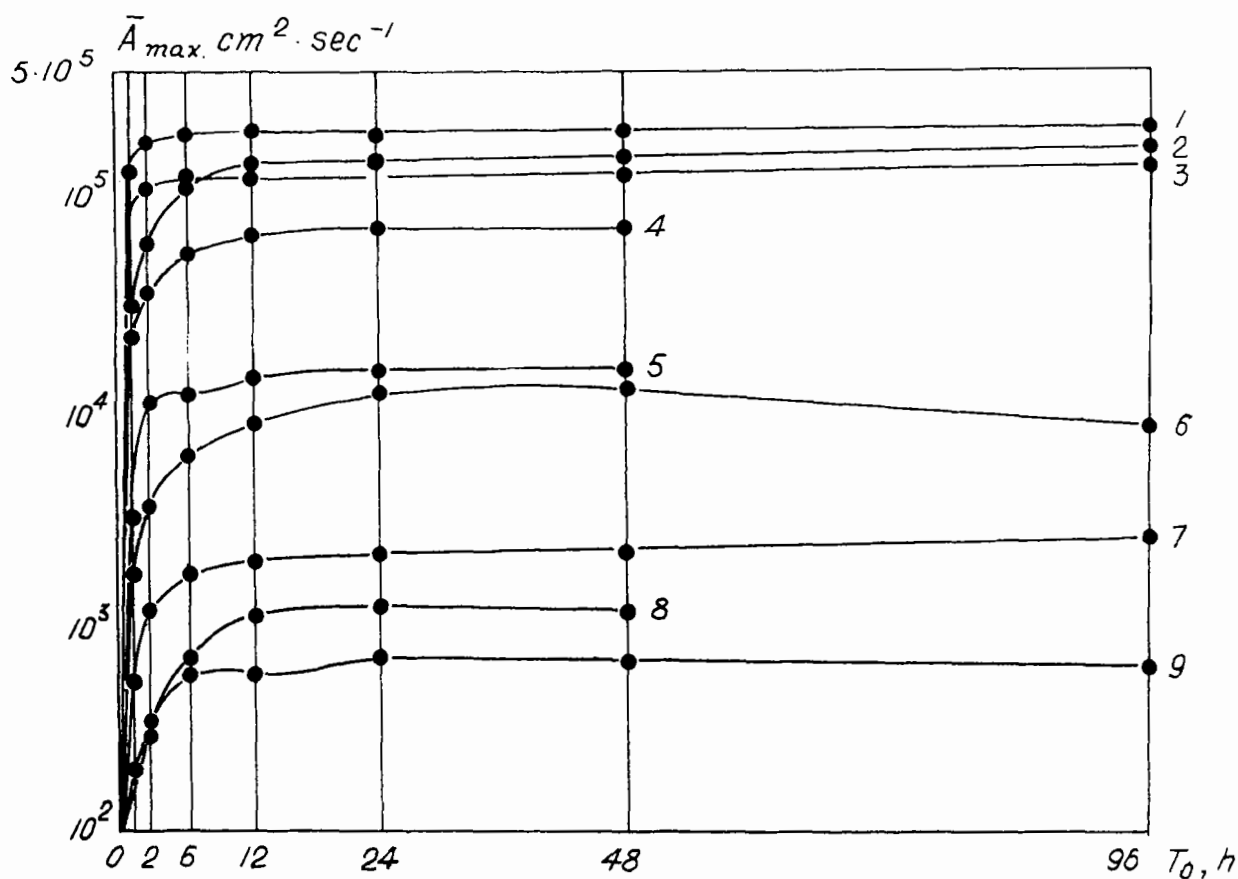


Figure 12. Fluctuations of averaged maximal coefficients of horizontal turbulent exchange of motion quantity (A_{\max}) due to the increase of averaging period (T_0) at atolls.

- 1 - southeastern coast of Cosmoledo, reef crest, station 19, horizon 11.5 m, depth of 12 m.
- 2 - southeastern coast of Cosmoledo, reef slope, station 18, horizon 12 m, depth of 20 m.
- 3 - eastern coast of Farquhar, station 4, horizon 20 m, depth of 50 m.
- 4 - southwestern coast of St. Joseph, station 15, horizon 15, depth of 32 m.
- 5 - Cosmoledo lagoon, at the Southeast Passage, station 20, horizon 2.5 m, depth of 3 m.
- 6 - western coast of St. Joseph, station 16, horizon 26.5 m, depth 27 m.
- 7 - eastern coast of Farquhar, station 6, horizon 17.5 m, depth of 18 m.
- 8 - eastern coast of Farquhar, station 5, horizon 8.5 m, depth 9 m.
- 9 - St. Joseph lagoon, station 17, horizon 2.2 m, depth of 3 m.

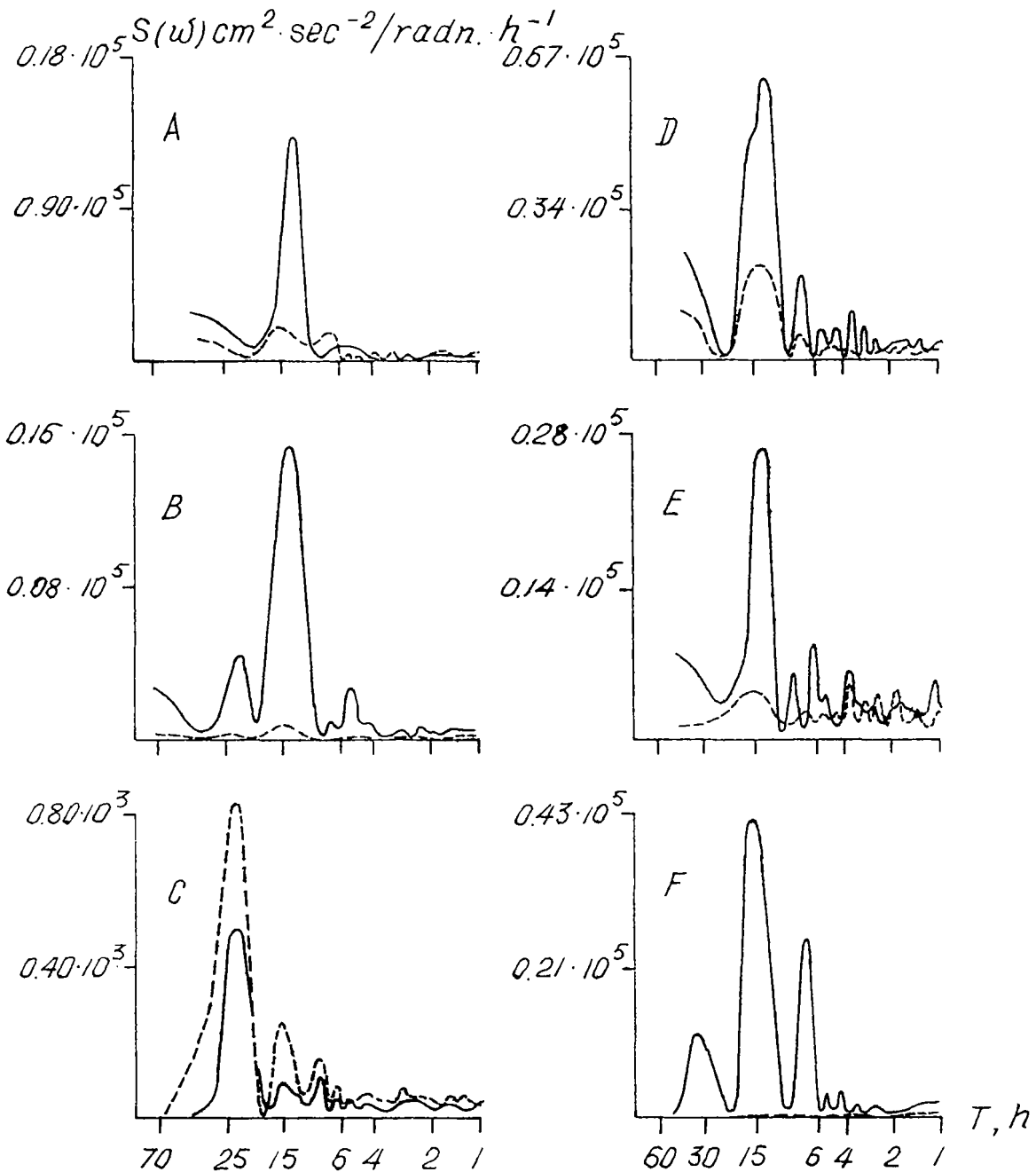


Figure 13. Function of spectral density of current rate pulse at atolls.

- A - reef slope at St. Joseph, station 15, horizon 15 m, depth 32 m.
- B - fore-reef platform at St. Joseph lagoon, station 16, horizon 26.5 m, depth of 27 m.
- C - St. Joseph lagoon, station 17, horizon 2.5 m, depth of 3 m;
- D - south-eastern coast of Cosmoledo, station 20, horizon 12 m, depth of 20 m;
- E - south-eastern coast of Cosmoledo, station 19, horizon 11.5 m, depth of 12 m;
- F - lagoon area adjoining Southeast Passage channel (Cosmoledo), station 20, horizon 2.5 m, depth of 3 m.

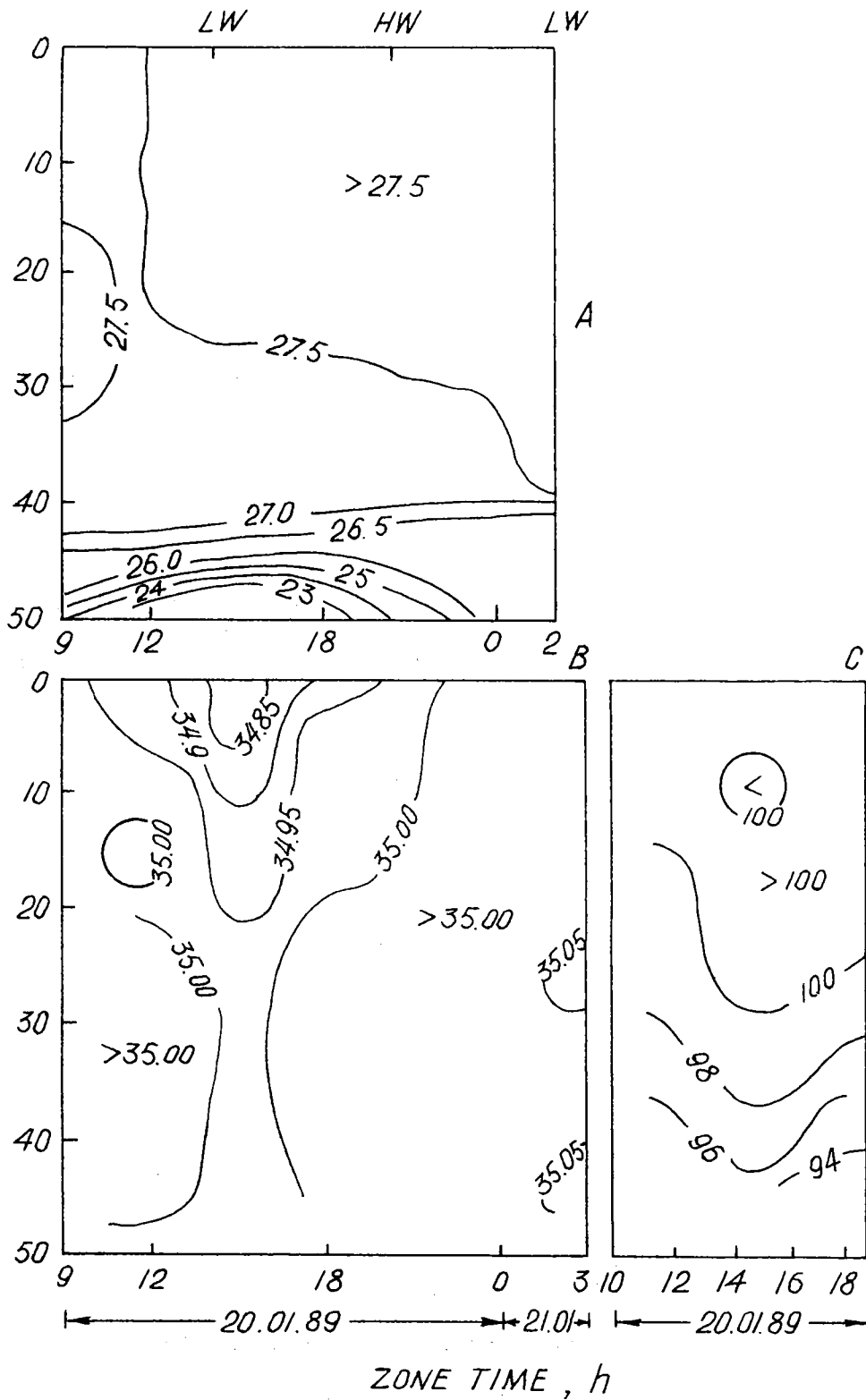


Figure 14. Temporal variability of temperature (A), salinity (B) and dissolved oxygen concentration (C) at Station 4, Farquhar.